

Serveur Académique Lausannois SERVAL serval.unil.ch

Author Manuscript

Faculty of Biology and Medicine Publication

This paper has been peer-reviewed but does not include the final publisher proof-corrections or journal pagination.

Published in final edited form as:

Title: Targeting iron-mediated retinal degeneration by local delivery of transferrin.

Authors: Picard E, Le Rouzic Q, Oudar A, Berdugo M, El Sanharawi M, Andrieu-Soler C, Naud MC, Jonet L, Latour C, Klein C, Galiacy S, Malecaze F, Coppin H, Roth MP, Jeanny JC, Courtois Y, Behar-Cohen F

Journal: Free radical biology & medicine

Year: 2015 Dec

Volume: 89

Pages: 1105-21

DOI: 10.1016/j.freeradbiomed.2015.08.018

Targeting iron-mediated retinal degeneration by local delivery of transferrin

Emilie Picard¹⁻³, Quentin Le Rouzic¹⁻³, Antonin Oudar¹⁻³, Marianne Berdugo¹⁻³, Mohamed El Sanharawi¹⁻³, Charlotte Andrieu-Soler¹⁻³, Marie-Christine Naud¹⁻³, Laurent Jonet¹⁻³, Chloé Latour⁴, Christophe Klein⁵, Stéphane Galiacy⁶, François Malecaze⁶, Hélène Coppin⁴, Marie-Paule Roth⁴, Jean-Claude Jeanny¹⁻³, Yves Courtois¹⁻³, Francine Behar-Cohen^{1-3,7}.

1 INSERM, UMRS 1138, team Behar-Cohen, From physiopathology of ocular diseases to clinical development, Centre de Recherche des Cordeliers, Paris, France.

2 Université Pierre et Marie Curie-Paris 6, Centre de Recherche des Cordeliers UMRS 1138, Paris, France.

3 Université René Descartes, Centre de Recherche des Cordeliers UMRS 1138, Paris, France.

4 INSERM, U1043, Toulouse, France; CNRS, U5282, Toulouse, France; Université de Toulouse, UPS, Centre de Physiopathologie de Toulouse Purpan (CPTP), Toulouse, France.

5 INSERM, U1138, CICC, Université René Descartes Sorbonne Paris Cité, Université Pierre et Marie Curie Paris, Centre de Recherche des Cordeliers, Paris, France.

6 INSERM U563, Centre de Physiopathologie de Toulouse Purpan, Toulouse, France; Department of Ophthalmology, Purpan Hospital, Toulouse, France.

7 Jules Gonin Ophthalmic Hospital, Lausanne, Switzerland.

Corresponding author:

Tel: +33 1 44 27 81 82; Fax: +33 1 44 27 81 77;

E-mail: emilie.picard@crc.jussieu.fr

Running title:

Transferrin protects against neurodegeneration

Keywords

Neurodegenerative diseases, Neuroprotection, Iron, Oxidative stress; Inflammation, Transferrin

Nonstandard abbreviations used:

AMD: age-related macular degeneration; ET: electrotransfer; IVT: intravitreal; MC: microglial cell;

RPE: retinal pigment epithelium; Tf: transferrin; PR: photoreceptor

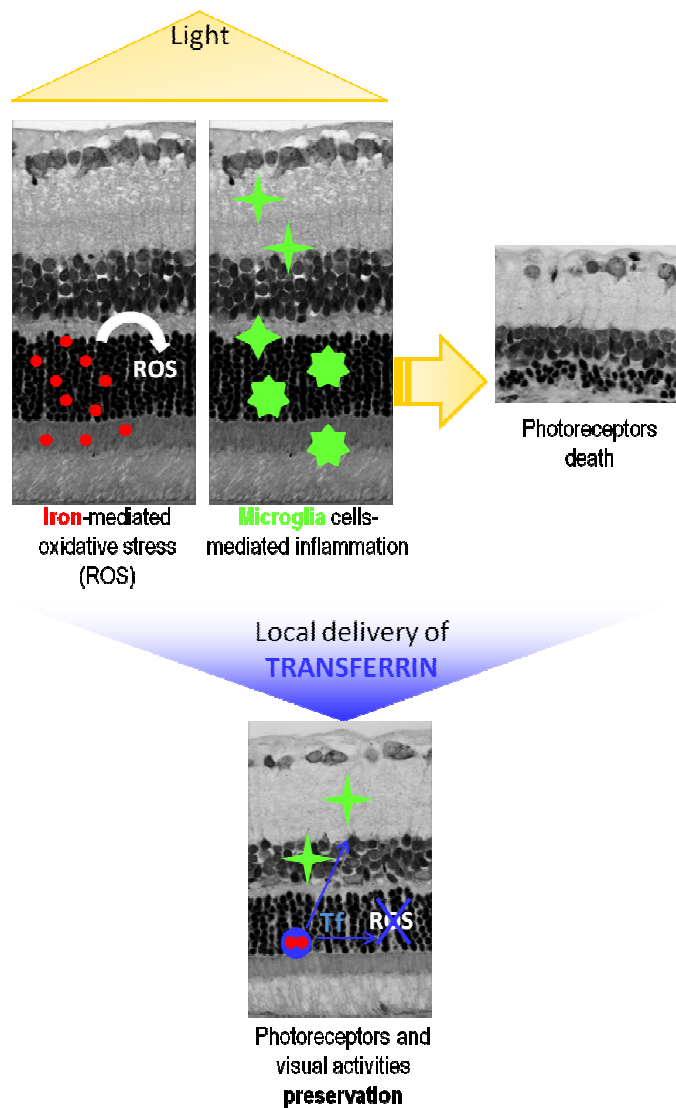
Conflict of interest

The authors declare that they have no conflict of interest.

Highlights:

- Transferrin injection in the eye has no deleterious effect on retinal structure
- Local delivery of transferrin protects photoreceptors and preserves retinal electrophysiological activities in light-induced retinal degeneration model
- Protective mechanisms of transferrin result from control of iron-induced death decrease and modulation of inflammation
- Intraocular administration of transferrin has therapeutic potential in retinal degenerative diseases

Graphical abstract:



ABSTRACT

Iron is essential for retinal function but contributes to oxidative stress-mediated degeneration. Iron retinal homeostasis is highly regulated and transferrin (Tf), a potent iron chelator, is endogenously secreted by retinal cells. In this study, therapeutic potential of a local Tf delivery was evaluated in animal models of retinal degeneration.

After intravitreal injection, Tf spread rapidly within the retina and accumulated in photoreceptors and retinal pigment epithelium, before reaching the blood circulation. Tf injected in the vitreous prior and, to a lesser extent, after light-induced retinal degeneration, efficiently protected the retina histology and function. We found an association between Tf treatment and the modulation of iron homeostasis resulting in a decrease of iron content and oxidative stress marker. The immunomodulation function of Tf could be seen through a reduction in macrophage/microglial activation as well as modulated inflammation responses. In a mouse model of hemochromatosis, Tf had the capacity to clear abnormal iron accumulation from retinas. And in the slow P23H rat model of retinal degeneration, a sustained release of Tf in the vitreous via non-viral gene therapy efficiently slowed-down the photoreceptors death and preserved their function.

These results clearly demonstrate the synergistic neuroprotective roles of Tf against retinal degeneration and allow identify Tf as an innovative and not toxic therapy for retinal diseases associated with oxidative stress.

INTRODUCTION

Oxidative stress and inflammation are recognized as major pathological processes in neurodegenerative diseases and iron is identified as a catalyzer of both processes (1-3). In the retina, iron is essential for photoreceptors (PR) activity as it is a cofactor of phototransduction enzymes (4-5). Iron content within the retina is generally controlled through locally expressed iron-related proteins (6-7). Nevertheless, iron excess can be found in the retina of elderly people (8) and is known to accumulate in retinal diseases (2, 9). For instance, in age-related macular degeneration (AMD), the common leading cause of blindness in industrialized countries, iron deposits can be found in PR segments, retinal pigment epithelium (RPE) and in drusen (sub-RPE deposits characteristic of AMD) (10). Moreover, increased iron concentration level are usually detected in the aqueous humor AMD patients (11). Free iron is shown to be highly toxic for PR (12), which loss lead to irreversible damage and thus to blindness. Similarly, we showed that iron accumulation and alteration of iron metabolism are both correlated with the progression of PR degeneration in animal models of retinal degeneration (rd10 mice and Royal College of Surgeons (RCS) rats) (13-15). Therefore, iron chelation allowing the removal of excess iron may very likely be a therapeutic target (16-17). Indeed, the use of chemical iron chelators such as deferoxamine and deferiprone administered by systemic or oral routes, were reported to be efficient in preventing PR death in animal models of retinal degeneration (14, 18-21). Nevertheless, the long-term systemic delivery of iron chelator may cause refractory iron depletion and may not be the best treatment option especially in elderly patients frequently suffering from anemia (22-23).

Our previous investigations showed that human transferrin (Tf), whether continuously expressed or administered intraperitoneally, preserve more than 60% of PR from death in rd10 mice (24-25). Indeed, Tf, the main iron transporter, is a natural iron chelator essential for homeostasis control (24, 26). Our study is the first attempt to directly injected an iron chelator into the eye. We performed intravitreal injections of human Tf in two different rat models of retinal degeneration and subsequently analyzed the pathways involved in its protective effect. We first used a light-induced retinal degeneration model in which oxidative stress is prominent (27-28). This allowed us to screen the optimal doses, the administration routes of Tf and its toxicity threshold. We simultaneously evaluated

the effects of Tf on iron metabolism, apoptosis and inflammation responses. In a second step, we used P23H rats suffering from slow retinal degeneration and used a non-viral gene therapy to evaluate whether sustained intra-ocular Tf production could delay the inherited degeneration.

This study highlights the therapeutic potential of local delivery of Tf on neuronal loss, oxidative stress and inflammation, the pathological features commonly observed in neurodegenerative diseases.

RESULTS

Time-related distribution of transferrin after intravitreal injection

We used Tf labeled with fluorochrom Alexa 488 (Tf-Alexa) to follow the fate of Tf in the rat retina after intravitreal (IVT) injection. Two hours after injection, Tf-Alexa could be detected throughout the retina, and was localized in retinal capillaries (arrowhead) and in the retinal pigment epithelium (RPE) (Figure 1A, left panel). A combination of Müller glial cells marker (Figure 1A, middle panel) with Tf-Alexa allowed us to show that Tf-Alexa was present along those cells, with largest concentrations in their end feet facing the vitreous (Figure 1A, right panel). Confocal microscopy conferring higher resolution allowed us to localize Tf-Alexa in microvillousities of RPE (Figure 1B) and in the inner and outer segments of rod PR (Figure 1C). Tf receptor 1 and TfR2 were widely expressed in the retina (26, 29). Tf-Alexa was co-localized with TfR1 in the inner plexiform layer (IPL), outer plexiform layer (OPL), inner segments (IS) and RPE (Figure 1D), and with TfR2 in IPL, ONL and IS (Figure 1E). Six hours after injection, Tf-Alexa had the same pattern, and was additionally detected within choriocapillaries (Figure 1F).

We used a specific transferrin (Tf)-ELISA assay to quantify Tf levels in ocular fluids and tissues after IVT injection of human Tf in rat eyes. ELISA assays were performed at 6, 24 hours and 7 days after injection (Figure 1G-H). When comparing Tf content 6 and 24 hours after injection, we observed a significant decrease of 67.3% in the neural retina and of 82.6% in the eye cup (Figure 1G). In ocular fluids, Tf concentration was higher in aqueous humor than in the vitreous, and increased with time (Figure 1H). Tf levels measured in the systemic circulation were of 56.6 ng/ml \pm 0.32 and 46.5 ng/ml \pm 5.77, 6 and 24 hours after injection. Finally, Tf was undetectable in both, eyes and plasma 7 days

after injection. These data indicate that IVT injected Tf reach the retina in a short amount of time and most likely via the Tf receptor 1. It subsequently accumulate in RPE cells and finally disappear through choroidal blood circulation.

Transferrin intravitreal injection has no deleterious effect on normal retina

We injected Tf in vitreous of rats and analyzed the retina and its histology 7 days later. Some rats obtained a single injection and others received a second injection 7 days after the first one. *In vivo* optical coherence tomography (OCT) imaging revealed no retinal structure modifications after one or two injections (Figure 2A). We used OCT pictures to measure ONL thickness which is usually correlated to PR nuclei number, and observed no differences among control not injected rats, and animals injected once or twice with Tf (Figure 2B). Moreover, when compared to eyes from control rats, rat eyes injected twice with Tf showed no substantial histological modifications in any layer (Figure 2C). Finally, an analysis of ONL thickness on sections crossing the optic nerve showed no significant difference between control and treated rats (Figure 2D) and thus confirm results obtained from OCT recording.

Transferrin intravitreal injection protects photoreceptors nuclear layer

Light-induced damage is a commonly used model to evaluate neuroprotective drugs on PR degeneration (28, 30-31). We injected Tf in the vitreous directly after a dark adaptation period of 18 hours. We further exposed the rats to intense light during 24 hours. We performed morphological analysis 8 days after light exposure using OCT recordings as well as histological semi-fine sections. OCT images realized at superior pole of rats injected with control solution (BLE group) showed a reduction in ONL thickness. Tf treatment (TfLE group) seemed to preserve the retina against light effects (Figure 3A). The ONL thickness measured on OCT images (Figure 3B) showed a significant decrease of 56% in BLE rats as compared to rats neither injected nor exposed to light (NLE group). There was no significant difference in ONL between TfLE rats and NLE rats. Histology confirmed OCT observations and measurements (Figure 3C-D). The most severe light-induced damage of BLE retinas was been observed occurring close to the optic nerve and especially on the superior side. The

rats treated with Tf had a preservation of ONL, IS, OS and RPE as compared to BLE rats (Figure 3C). ONL thickness measured throughout the retina showed that 70% of the PR nuclei at the superior pole and 92% at the inferior pole were protected with Tf injection (Figure 3D).

Transferrin preserves PR structures and functions.

We assessed apoptotic cells by TUNEL staining on eye cryosections to better evaluate the preservation of PR nuclear layer with Tf treatment (Figure 4A). One day after light exposure, many TUNEL positive PR were present in the ONL of BLE rats. TUNEL intensity staining quantification in ONL throughout the retina demonstrated a significant reduction of 40% in the number of apoptotic PR in TfLE retinas as compared to BLE (Figure 4B). We stained rods by rhodopsin immunodetection and cone by lectin-peanut labeling 8 days after light exposure to confirm Tf-treatment PR morphological preservation. When compare to unexposed eyes (NLE), BLE retinas had a close to complete loss of both types of PR (Figure 4C, middle panel), whereas Tf-treatment retinas (TfLE) showed preserved structures in both rods and cones (arrows) (Figure 4C, right panel).

We performed full-field electroretinograms 16 days after light-exposure to determine whether the above-described results correlate with the maintenance of retinal function. In scotopic conditions, light-exposure drastically lowered a- and b-wave amplitudes in BLE rats, meaning a decreased rod-driven response (Figure 4D). With Tf treatment, these amplitudes were significantly higher compared to BLE group (Figure 4D). In an extensive analysis in the flash intensity ranging from -0.5 to 0.47 $\log(\text{cd.s/m}^2)$, the mean a-wave amplitude of TfLE reached 55.18% of NLE, and the mean b-wave amplitudes in TfLE rats were 47% of NLE values. The protection of scotopic a- and b-wave amplitudes were confirmed by the mixed rod-cone responses recording (Supp. Figure 1). Tf significantly preserved 85% of PR response (a-wave amplitude; Supp. Figure 1A left panel), and 54.8% of internal retina response (b-wave amplitude; Supp. Figure 1A right panel) relative to unexposed rats. The time-to-peak for mixed ERG a- and b-waves were not statistically different in the three rat groups, in spite of a tendency toward a Tf-induced preservation of implicit times (Supp. Fig 1B). Following a rod-suppressing light adaptation, the photopic b-wave responses (Figure 3E, left panel), specific for cone responses were recorded. Nonetheless, the amplitudes did not differ between

BLE and TfLE. These were lower compared to NLE. The implicit time (right panel) was significantly longer in BLE as compared to NLE, and significantly restored in TfLE rats. To better characterize this effect on cones, we quantified cones in overall retina (Figure 4F). Eight days after light exposure, there was a 43% cone loss in BLE retinas and a 23% cone loss in TfLE retinas when expressed as % of cones within the control NLE group. In conclusion, IVT injection of Tf was effective in protecting cones and rods from death and allowed to preserve the physiological activities of the retina against light-induced retinal damages.

Iron metabolism deregulation in light-damage retina is restored by transferrin IVT injection

Previously publications showed that intense light-exposure induces an acute and rapid modification of iron metabolism that persists for several days after light damage (25, 32). To evaluate the effects of Tf in iron homeostasis, we investigated the regulation of iron-related genes and proteins as well as the iron content and distribution after light-exposure.

One day after light exposure, quantitative RT-PCR (Figure 5A) on neural retinas monitored expression of genes related to iron transport (*Tf* and *TfR1*), storage (heavy and light Ferritins (*FtH* and *FtL*)), export (Divalent metal transporter 1 (*Dmt1*), Ferroportin (*Fpn*) and Ceruloplasmin (*Cp*)), and regulation (*TfR2*, Human hemochromatosis protein (*Hfe*) and Hemojuvelin (*Hjv*)). Except for *Cp* and *FtL*, transcripts of all analyzed iron-related genes significantly decreased in BLE rats as compared to control NLE rats. In Tf treated retinas, the expression of *Tf*, *TfR1*, *Dmt1*, *Hfe* and *Hjv* mRNA was partially but significantly restored as compared to BLE retinas. The light-induced expression of *Cp* was significantly increased in TfLE rat retinas. Tf treatment had no significant effect on *FtH*, *FtL*, *Fpn* and *TfR2* transcription when compared to BSS injected rat retinas.

Using immunohistochemistry, we observed the expression of the two ferritins and TfR1 proteins at different time points after the light-exposure (Figure 5B-D). The expression of these proteins are known to correlated with the retina iron content, regulated by iron regulatory proteins IRP1 and IRP2 (25, 33). One day after light exposure, no modification of the two ferritins staining was observed in BLE and TfLE treated groups as compared to NLE (data not shown). At day 3 and 8, ferritin staining intensity was increased in the retina of BLE rats (Figure 5B-C, central column) whereas no obvious

modification was observed in the retina of TfLE rats when compared to NLE rats (right compared to left column). While TfR1 decreased in the retinas of BLE rat (Figure 5D, central panel), it remained similar to the retinas of NLE rats in the TfLE rat eyes (right panel). Given the previous results, we explored whether Tf treatment had an impact on iron accumulation in the retina, and revealed non-hemic iron using Perls Prussian blue reaction intensified with diaminobenzidine (Figure 5E). Iron accumulated in the outer retina of BLE rat at day 3 and 8 after light exposure (Figure 5E, middle panel). Such an accumulation could not be detected in the retinas of TfLE rat at any time point (Figure 5E, right panel). This was confirmed with the total non-heme iron quantification determined in neural retinas at 8 days after light exposure (Figure 5F) and demonstrates that Tf significantly prevent free iron content increase. To investigate the effect of Tf on oxidative stress, we assessed heme oxygenase (*Hmox1*) mRNA expression using qPCR on neural retina one day after light-exposure. Light-induced iron overload significantly increases *Hmox1* in the BLE group. This upregulation was less important in the retinas of rats treated with Tf (Figure 6). These results demonstrated that IVT of Tf allows a rapid and efficient control of iron homeostasis thereby avoiding iron accumulation and oxidative stress.

Light-induced retinal inflammation is controlled by transferrin.

Microglial cells (MC), specific macrophage/monocyte of the retina, are activated by light exposure and migrate towards PR debris (34-35). We used ionized calcium-binding adapter molecule (Iba1) and CD68 as markers to reveal macrophage/monocyte. Both are constitutively expressed but CD68 is restricted to lysosomal membranes of non-activated cells, and is expressed in the cytoplasm of activated cells, allowing the discrimination of the activation state at 1, 3 or 8 days after light-induced damage (Figure 7A-H). We localized non-activated MC in the inner retina of NLE rats (arrow, Figure 7A). Twenty-four hours after light-damage, Iba1 positive cells had migrated towards the outer retina in both rats and most of them were CD68- (arrows, Figure 7B-C). At 3 days, numerous round Iba1+ cells increased in outer retina in BLE and TfLE rats (Figure 7D-E). Higher magnification of subretinal space revealed that the Iba1+ cells were CD68+ in BLE rats, while Iba1+/CD68- cells represented the majority in TfLE rats (Figure 7D2-E2). CD68+/Iba1+ intensity ratio quantified in cells staining in the outer retina (Figure 7F) show that the majority of Iba1+ cells were also CD68+ in BLE rats. This was

true only for half the cells within the TfLE group. At 8 days (Figure 7G-H), numerous Iba1+/CD68+ amoeboid cells remained in the outer part of retina of BLE rats (arrows), while Iba1+ non-activated cells were localized in the inner retina in the TfLE group (arrowheads).

To get a better picture of the effect of Tf on light-induced retinal inflammation, we performed a PCR array on 84 genes of inflammatory mediators on the neural retina, 1 day after light exposure. In the BLE group, 34 genes were up-regulated and 13 down-regulated when compared to the NLE control group. When comparing the TfLE group to the NLE group, 42 genes were up-regulated and 9 down-regulated (Table 1). Figure 8 shows gene distribution differentially regulated in TfLE when compared to BLE according to their p-value versus fold change. *Ccl5*, *Ccl6*, *Cxcl3*, *Cxcl5*, *Il9* genes were significantly upregulated, whereas *Il23r*, *Il22*, *Il1rap* and *Faslg* were down-regulated. List of genes modified by one-third by Tf injection are indicated in Supplemental Table 2. All these data indicate that IVT of Tf control inflammatory cell activities through the modulation of inflammatory mediators induced during light-exposure.

Transferrin has a long-term effect and efficacy in advanced disease models.

To evaluate the effectiveness of Tf in animals models presenting pathogenic characteristics such as iron accumulation, photoreceptors degeneration and long-term disease evolution: 1- we administered Tf treatment when part of the retina had already been damaged through light exposure; 2- we induced sustained expression of Tf, via ciliary muscle electroporation of a plasmid encoding human Tf, in the P23H rat model of slow retinal degeneration; 3- we tested the efficacy of Tf in removing iron deposits from the retina of the *Bmp6*^{-/-} mouse genetic model presenting iron overload.

1- Effect of IVT Tf treatment on partially degenerated retina. In retinal disease, PR death begins before diagnosis, and therefore prospective treatments would have to be initiated in deleterious conditions. The onset of light-induced retinal damage is rapid, occurring in about 2 hours after light exposure. Once started PR degradation continues for a 2 days period (36). To demonstrate that Tf can protect PR even after the degenerative process has begun, we performed IVT injection subsequent to light-exposure. Eight days after the injection, ONL was mainly destroyed in BLE rats (Figure 9A, arrows). Throughout the entire BLE rat retina, the mean ONL thickness was 12.5% of the NLE (NLE:

39.43 μm \pm 1.10; BLE: 5.94 μm \pm 0.40) (Figure 9B). In the TfLE group, Tf was not able to protect the PR layer at the superior pole, which was largely destroyed. However, relative to NLE rats, 50% of PR nuclei were preserved in the inferior pole (mean ONL thickness of NLE: 40.43 μm \pm 1.51; TfLE: 20.3 μm \pm 2.72). This suggests that Tf injection may have a protective effect on partially damaged retinas.

2- Sustained production of Tf by gene therapy in slow retinal degeneration model. IVT injections are routinely used for eye treatment. In the context of chronic diseases such as dry AMD, frequent intraocular injections may contribute to reduce treatment compliance. Our laboratory has developed a non-viral gene therapy strategy based on ciliary muscle cells transduction via electrotransfer (ET) thereby serving as a biofactory for sustained production of therapeutic proteins in the vitreous (37). Using a disposable device and a minimally invasive procedure, this gene therapy technique can be applied to secrete proteins of any molecular weight for several months (38-39). We produced pVAX1-Tf plasmid through subcloning the cDNA of human Tf in a pVAX1 backbone under a cytomegalovirus- β promoter which is known to be efficient for ET protocol (38). We transfected human immortalized RPE cell line (ARPE-19) that does not synthesize Tf with pVAX1-Tf and immunoblotted the culture media. The size of the produced Tf was similar to Tf isolated from human plasma (Supp. Figure 2A). We used Tf-ELISA assay to determine the amount of Tf produced in the rat eye 3 days after after ET. We detected human Tf in all compartments of the eye, including the vitreous, aqueous humor and neural retina as well as the eye cup (Supp. Figure 2B). When performing retinal histology 12 days after ET, we did not observe any difference in eyes ET with empty pVAX1 as compared to control eyes and did not see any variation of ONL thickness for eyes in which we induced Tf production (control: 45.11 μm \pm 1.82; ET pVAX1: 45.97 μm \pm 1.92; ET pVAX1-Tf: 43.03 μm \pm 1.31) (Figure 10A-B). We performed ET 3 days before exposing rats to light to evaluate *in oculo* the efficacy of produced Tf on PR degeneration (Figure 10C-D). ET of empty pVAX1 plasmid did not have a significant impact on light-induced retinal damage (mean of ONL thickness of rat exposed to light (LE): 18.78 μm \pm 0.69 compared to rat injected with pVAX1 and exposed to light: 15.71 μm \pm 0.89), whereas plasmid induced-Tf allowed to preserve 67% of ONL thickness as compared

to rats not exposed (rat injected with pVAX1-Tf and exposed to light: $30.10\mu\text{m} \pm 2.08$ versus control not light-exposed figure 10B).

We further tested the efficiency of Tf production in the P23H rhodopsin transgenic rat model of gradual PR loss, a model of autosomal dominant retinitis pigmentosa (40). We induced ET with pVAX1-Tf or empty-plasmid when PR loss had already begun (4 weeks-old rats) and collected the eyes 4 weeks later. Eight week-old P23H control rats presented nearly one fourth of ONL thickness as compared to control wild-type rats (Figure 10E-F compare to 10A-B) (P23H: $12.83\mu\text{m} \pm 0.72$). Synthesis of Tf in P23H eye significantly preserved PR nuclei as compared to P23H eyes electrotransferred with empty pVAX1 (P23H rats ET with pVAX1: $10.61\mu\text{m} \pm 1.17$; P23H rats ET with pVAX1-Tf: $16.15\mu\text{m} \pm 0.71$) (Figure 10 E-F). These results demonstrate that Tf expressed in the eye via gene therapy can protect the retina from retinal degeneration whether acute or progressive.

3- Iron removal in a mouse model of iron retinal overload. In AMD, iron accumulates in RPE, drusen and outer segments of PR (8). We used mice knock-out for the Bone Morphogenetic Protein 6 (*Bmp6*) gene, a model of hemochromatosis to validate the effect of Tf in reducing iron deposits in the retina. By binding with its specific receptor, BMP6 protein activates transcription of the hepcidin gene. This peptidic hormone blocks iron cellular exportation by activating ferroportin proteolysis. In *Bmp6* KO mice eyes, we detected iron deposits in the RPE at 22 weeks and also in inner segments of PR in older mice (data not shown). *Bmp6* KO mice develop severe retinal degeneration by 41 weeks (41). We used 32 week-old mice already presenting iron overload in the RPE to test the efficacy of iron-removal by Tf (Figure 11A-B). We used two different protocols of Tf administration: 3 intraperitoneal injections per weeks over a one-month period, or a single IVT injection 7 days before eyes collection. As observed in Figure 11A, iron deposits on the basolateral side of RPE were partially removed with systemic infusion. Both treatment protocols significantly reduced iron deposits in the RPE by nearly 10% (IP BSS: 102.1 ± 2.6 ; IP Tf: 91.47 ± 2.35 ; IVT BSS: 105.5 ± 3 ; IVT Tf: 97.71 ± 3.74) (Figure 11B). Tf was efficient to remove iron accumulation.

DISCUSSION

In the present study, we investigated whether intravitreal injection of the endogenous iron chelator, transferrin, is efficient to prevent and protect PR against degeneration in several animal models.

The pathogenic role of iron is recognized in neurodegenerative retinal diseases and the use of iron chelators (deferrioxamine, deferiprone or deferasirox) has been already evaluated (42-45). Oral deferiprone has been the most studied drug in different murine models of retinal degeneration (hereditary, light- or iron-induced) and had a protective effect on PR (19-20, 46-47). However, in the absence of iron overload, systemic iron chelation therapy raises safety issues including chelator overdose toxicity, iron and other essential metal deficiencies as well as diseases associated with such metabolic imbalance. Ocular toxicity including cataract, maculopathy, and optic neuritis has been reported in patients treated with deferrioxamine or deferasirox during an extended period (48-50).

Aside from the synthetic (as deferiprone or deferasirox) and phytochemical chelators (curcumin, R-lipoic acid), Tf is an endogenous and potent iron chelator locally produced by ocular cells. Its main property is to control iron content in order to avoid any free labile iron, known to be a source of oxidative stress and cell death. Systemic administration of Tf exerted strong neuroprotective effects on rodent models of retinal dystrophies (14), positioning Tf supplementation as a therapeutic option for patients with retinal degeneration. For clinical use, parenteral administration is not adapted, particularly if long-term treatment is envisaged. We therefore conducted this extensive study to explore and better understand the effects of Tf administered locally through an intravitreal route. When injected into the vitreous, Tf rapidly penetrated into the retina through Müller glial cell end feet at the vitreous border. The presence of Tf in choroidal capillaries within a few hours after its intravitreal injection suggests that Tf follows a transretinal elimination route through Tf-receptors localized on vascular endothelial cell. Indeed, we detected Tf in plasma already 6 hours and up to 7 days after IVT injections, demonstrating a quick turn-over of Tf in the retina. This led us to inject Tf just before or just after a 24 hours continuous light exposure.

In acute models of light-induced retinal degeneration, PR death occurred within one day and was associated to retinal inflammation and iron homeostasis remodeling (14, 32, 35). The local administration of Tf before light exposure, allowed morphological preservation of 70% of PR cells

(Figure 3C, 4C). Electroretinograms recording allowed us to confirmed the functionality of PR cells with 50% of rod-driven electrical responses and an improved cone response time, indicating preservation of cone and rod responses and synaptic connections with retinal neurons (Figure 4D-F). These protective effects of IVT of Tf were associated with a decrease in apoptotic cells (Figure 4A) and a reduction of oxidative stress-induced heme oxygenase expression (Figure 6).

Pre-treatment with Tf also protected against the early iron imbalance induced by light exposure, as detected on iron-related genes expression 1 day, and on iron retinal tissue staining 3 days after light exposure (Figure 5). Indeed, the retinal expression of iron-related proteins regulated through the IRP/IRE system, dependent on the intracellular iron status, was modified rapidly during light exposure (25). Here, we propose that pre-treatment with Tf avoids iron retinal overload through the down-regulation of *TfR1*, *Fpn*, ferritins, and *Dmt1* mRNA. Similarly, oral deferiprone and deferoxamine regulated Hmox1, TfR1 and ferritin expression in models of retinal degeneration (19-21, 46-47). Tf exerted a much stronger regulation of other iron-related gene expressions, *Tf*, *Cp*, *HFE*, and *HJV*, which do not depend on IRP/IRE systems. Heparin is a peptidic hormone synthesized in the retina that enhances ferroportin proteolysis under iron excess and inflammation, decreasing iron released (51-52). Its transcription is controlled by several signaling pathways, including Hemojuvelin (HJV)/BMP-6, IL6 and TfR2/HFE (53-54). Previously, Hadziahmetovic M. et al. demonstrated that IVT injection of Tf rapidly activated ERK1/2 signaling pathways through Tf/TfR2/HFE binding, which reduced iron export (55). One day after light exposure, *Hfe*, *TfR2* and *Hjv* expression were down-regulated in the retina. This may decrease Heparin transcription and enhance iron release and PR death. The IVT injection of Tf prevented the light-induced *Hfe* down-regulation, which potentially enhanced the TfR2-HFE-Heparin pathway, and thus decreased iron exportation from cells. The role of TfR2 in iron metabolism is not fully understood, and its intracellular regulation, known to be independent of IRP/IRE system is not well characterized (56). In the retina, TfR2 is expressed in all nuclear layers, Tf injected co-localized with TfR2 in IPL, ONL and inner segments (Figure 1D-E). Recently, Wysokinski et al. showed an association between a polymorphisms of the *TfR2* gene and the occurrence of AMD in obese patients (57). And Tf neuroprotective effect has also been demonstrated to depend on TfR2 binding (58-60). Thus, the local delivery of Tf, not only binds toxic free iron but

exerts a complex and interesting regulation of several proteins involved in retinal iron trafficking, resulting in a further reduction of iron-mediated oxidative toxicity.

Another mechanism of Tf neuroprotective effects on light-induced retinal degeneration is related to the regulation of retinal inflammation. Studies already demonstrated that Tf modulated the cytokines profile in animal models of inflammation (61-62) and reduced the ageing-associated immunologic decline in mice (63). Tf was also shown to be efficient in an ocular model of intraocular inflammation (64). In our model, the intense cold white LED exposure induced an early retinal expression of genes involved in MC/macrophages recruitment (day 1) (*Ccl2*, *Ccl17*, *Ccl12*, *Ccr2*, *Ccr4*, and *Il1a*). This was followed by the massive infiltration of activated Iba1+ cells in the outer retina at 3 days (65-66) and the possible recruitment of circulating monocytes attracted by molecules up-regulated in the illuminated retina (*Csf1*, *CD14*, Interleukins, Toll-like receptors group, Cxcl chemokines and Cxcr receptors family genes) (67). Tf treatment induced a reduction of CD68 intensity staining in Iba1 positive cells (Figure 7F) suggesting deactivation of MC/macrophages in the retina, known to be neurotoxic for PR and RPE cells (68-70). Tf also reduced retinal inflammation by the up-regulation of the anti-inflammatory cytokines Il1rn and Il9 (71) and the down-regulation of pro-inflammatory cytokines Ccl1, Il1rap, Il22, Il23r (72-73). This supports an additional neuroprotective mechanism of Tf in relation with inflammatory responses. In this experiment, the modulation of cytokines profile expression paralleled the iron-related genes modification and the exact relation between these two mechanisms remains to be studied.

There are a number of considerations to use local delivery of iron chelator in a context of retinal disorders such as dry AMD. Beyond retinal protection, PR preservation in deleterious condition such as iron overload and chronic PR loss needed to be investigated. In this study, we showed that Tf not only protected the retina prior to light-exposure but was still partially effective after light exposure. Mechanisms could include reduction of reactive oxygen species production, iron accumulation, and lipids peroxydation. The therapeutic potential of Tf is also suggested by its ability to “clear” the outer retina and RPE from accumulated iron (Figure 11). Thus Tf could be administered not only for prevention but also to delay ongoing retinal degeneration. Because the half-life of Tf was short, and

retinal degeneration diseases are chronic diseases needing treatment over long period, a non-viral gene transfer technique was used to produce Tf locally in a sustained manner. The ciliary muscle electrotransfer of a plasmid encoding Tf not only showed a significant effect preventing PR degeneration in the acute light-induced retinal degeneration model (Figure 10 C-D) but also demonstrated a protective effect in a genetic model of slow retinal degeneration, the P23H rat (Figure 10 E-F). This indicates that the slow and continuous intraocular release of Tf may very likely be beneficial to treat progressive retinal degeneration diseases.

CONCLUSION

Many strategies are being developed to delay retinal degeneration and proving their efficacy in clinical trials is a real challenge. Whatever the cause of retinal degeneration, oxidative stress is involved in PR death and, in this context, iron neutralization is one of the strategies present in all neurodegenerative diseases. However, due to the redox activity of iron, it is important to consider whether iron chelators can provide the cellular specificity required to remove excess of iron from the appropriate tissue, without affecting systemic iron homeostasis. Here, we demonstrated that the local administration of Tf, the endogenous iron chelator naturally present in the eye, responded to this criteria. We showed that Tf protects PR against intense cell-death and preserves retinal functions through several mechanisms: oxidative stress, iron homeostasis balance, inflammation control and reduction of apoptosis. Therefore, we propose local ocular Tf administration as a high benefit/risk ratio therapeutic candidate to be evaluated to limit PR cell death in patients and with further potential applications including degenerative retinal diseases such as dry AMD.

METHODS

Animals

Animals were fed with a standard laboratory diet and ad libitum tap water in a temperature-controlled room at 21-23°C. The cyclic light environment consisted of 12 hours light per day (6am-6pm). Animals were sacrificed by carbon dioxide inhalation. All experimental procedures in rats were submitted and approved by the local ethics committee European Council Charles Darwin, University

Paris Descartes. Experiments were performed in accordance with the Association for Research in Vision and Ophthalmology (ARVO) statement for the use of animals in Ophthalmic and Vision Research.

Photic injury

During the 3 weeks prior to light exposure, to reduce PR sensibility variability between rats, Wistar rats (7 to 10-months old) (Janvier laboratory, Le Genest St Isle, France) were adapted in ventilated cages at the bottom rows of the rack, where the level of light was controlled below 250 lux (74).

The day before light exposure, rats were dark-adapted 18 hours from 6 pm. The next day, pupils were dilated with 1% atropine (Alcon, Novartis, Rueil Malmaison, Fr) under dim light, and rats were isolated in separate cages containing enough food for one day. Then light-exposure was performed with commercial cold white LED panel generating 2,300 lumens during 24 hours. The LED panel was placed above 8 transparent cages, placed on white surfaces, leaving enough space for air circulation and constant temperature maintenance at 23°C. The luminance measured at the rats' eyes position was 6,500 lux (Photometre DT-8809A, CEM, China). After light exposure, rats were replaced under cyclic light (12h/day, 250 lux) for 1, 3, 8 or 16 days. Control animals were also dark adapted, and then returned to rearing cyclic light conditions.

Rats were randomly separated into 3 groups (n= 4-5 rats per group): a control group not exposed to light and untreated (NLE), a group treated with intravitreal injection of sterile saline buffer (BSS, Bausch and Lomb, Montpellier, Fr) and exposed to light (BLE), and a group treated with an intravitreal injection of human Tf solution and exposed to light (TfLE).

Intravitreal injections were performed after dark adaptation period under dim red light, or after light exposure under normal light condition. Lyophilized apotransferrin (iron free transferrin (Tf)) isolated from human plasma was dissolved in sterile BSS solution at a concentration of 48mg/ml (T5391, Sigma Aldrich Chemical Co, Saint-Quentin en Yvelines, Fr). Rats were anesthetized using intramuscular injection of 35:25 mix of ketamine (Virbac, Carros, Fr) and xylazine (Bayer, Lyon, Fr) (1ml/100mg) and intravitreal injections (5µl,) were performed in inferior quadrant of both rat eyes using a 30-gauge needle under an operating microscope. This content was determined as the most

efficient to protect photoreceptors (data not shown). Rats were sacrificed at different time points after light exposure. For *in vivo* analysis and histology, rats were examined or sacrificed 8 or 16 days after light exposure. Additional time points were used for immunohistochemistry and RT-qPCR at 1, 3 or 8 days after light exposure.

Kinetic of transferrin eye distribution after intravitreal injection

At 6, 24 hours and 7 days after intravitreal injection of apotransferrin (5 μ l at 48mg/ml in BSS; 240 μ g), rats were sacrificed and eyes were enucleated, rinsed in 0.9% NaCl and dried. Ocular media and tissues were separated: aqueous humor and vitreous, cornea, iris/ ciliary body, neural retina, and RPE/choroid/sclera (eyecup). Retina and eyecups were analyzed individually whilst vitreous and aqueous humor from same eyes were pooled. Tissues were incubated in lysis buffer [15 mM Tris, pH 7.9, 60 mM KCl, 15 mM NaCl, 2 mM EDTA, 0.4 mM phenylmethylsulphonyl fluoride (PMSF) (Perbio Science, Brebiers, Fr)]. After four freeze/thaw cycles, lysates were centrifuged at 5,000g for 10 min and supernatants were stored at -20°C . Ocular fluids were diluted to a sufficient volume for assay. Human Tf was quantified by an antibody-sandwich ELISA as described (14).

Immunohistochemistry

Freshly enucleated eyes (n=3-4 per time point) (superior pole tagged with suture) were fixed for 2 hours with 4% paraformaldehyde (PAF, Inland Europe, Conflans sur Lanterne, Fr) in 1X phosphate-buffered saline (PBS, Gibco distributed by Life Technologies), washed with PBS, infiltrated in gradients sucrose series and then, mounted in Tissue Tek O.C.T. (Siemens Medical, Puteaux, Fr).

Immunohistochemistry was performed on 10 μ m-thick sections as previously described (14, 25). Cryosections were incubated with different primary antibodies: rabbit polyclonal anti-Tf receptor 1 (Serotec, Oxford, UK), rabbit polyclonal specific for the High and Light subunits of Ferritin (P. Santambrogio); rabbit anti-cellular retinaldehyde binding protein (CRALBP; J. Saari); rabbit anti-RPE65 (AbCys, Courtaboeuf, Fr); rabbit anti-ionized calcium-binding adapter molecule 1 (Iba1, Wako Pure Chemical Industries, Neuss, Germany); mouse anti-CD68 (Bio-Rad AbD Serotec GmbH, Colmar, Fr); goat anti- Tf receptor 2 (Genetex, Euromedex, Souffelweyersheim, Fr). Rods and cones

were respectively labeled with anti-rhodopsin (Rho4D2, R.S. Molday) and peanut agglutinin conjugated with fluorescein isothiocyanate (Sigma). Control sections were incubated with rabbit non-immune serum (Invitrogen, Cergy Pontoise, Fr) or without primary antibodies. The corresponding Alexa-conjugated secondary antibodies (Invitrogen) were used to reveal the primary antibodies, and sections were counterstained with 4,6-diamidino-2-phenylindole (DAPI; Sigma). The sections were viewed with a fluorescence microscope (BX51, Olympus, Rungis, Fr) or confocal microscope (LSM 510 laser scanning microscope Zeiss, Carl Zeiss, Le Pecq, Fr) and photographed using identical exposure parameters for all samples to be compared.

Quantification of cones number 7 days after the end of light-exposure was realized throughout the superior pole of retinal sections and reported to control rats as 100%. Microglia cells activation 3 days after end of light-exposed was determined in outer plexiform layer, outer nuclear layer and segments layers, identified after DAPI nuclei stain. Measurement of microglia/macrophages staining was performed on pictures (60X) taken in the overall retina with same exposure time. The rapport of CD68 intensity staining to total microglia cells revealed by Iba1 intensity staining was measured with ImageJ software.

Histology and outer nuclear layer thickness measurement

Oriented ocular globes were fixed with 4% PAF, 0.5% glutaraldehyde (LADD, Inland Europe, Fr) in PBS for 2 hours. After fixation, samples were washed, dehydrated and transferred into the infiltration solution of the Leica Histo-resin embedding kit (Leica, Nanterre, France) over night at 4°C. Samples were embedded in resin (Leica) and 5 µm thick sections passing through the optic nerve head were prepared along the superior and inferior pole of the eye using a microtome (Leica), stained with 1% Toluidin Blue solution. Sections were observed on a Leitz microscope and photographed with a Leica camera. Thicknesses of outer nuclear layer (ONL) were measured every 500 µm using Visilog 5.3 software (Noesis, Courtabouef, Fr). Histological sections measurements were performed across the whole retina, considering the inferior pole to 0 from -4,000µm of optic nerve and superior pole to 0 from 4,000µm of optic nerve. Thickness profiles along the retina were generated by averaging, for each distance, the values obtained for all eyes treated similarly to give a single value per group.

Optical Coherence Tomography

For *in vivo* analysis, rats were anesthetized, pupils were dilated and pictures of retinas of both rat eyes were performed at superior pole using spectral domain OCT (SD-OCT; Spectralis device; Heidelberg) adapted for small animal eyes. Each volume scan consisted of at least 100 B-Scans recorded at 30° field of view centered on the superior pole, which were used to measure retinal thickness across the scanned retinal area.

Electroretinography

Full-field ERG responses were recorded 16 days after the end of light exposure. Rats were dark-adapted over a period of 18 hours – for scotopic recordings – and anesthetized by an intramuscular injection of a mixture of ketamine and xylazine. The cornea was desensitized with a drop of oxybuprocaine (Novesine© Novartis Ophthalmics, Basel, Switzerland) and the pupils were dilated with a drop of tropicamide (Tropicamide©, Novartis Ophthalmics). Gold wire ring electrodes were placed on the corneas of both eyes and stainless steel needle electrodes inserted into the forehead served as working electrodes and references electrodes, respectively. A needle was subcutaneously inserted at the base of the animal tail for grounding. All these manipulations were performed under dim red light, without bringing the animal into ambient light after dark adaptation. Measurements were performed simultaneously in both rat eyes using the commercial Ganzfeld VisioSystem device (Siem Biomedicale, Nîmes, Fr). For scotopic electroretinograms in the dark-adapted state, flash intensities ranged from 0.0003 to 10 cd.s/m². Five flashes per stimulation intensity were applied at a 0.5 Hz-frequency, and corresponding responses were averaged. Flash duration was 10ms (–30 to 0 dB) except for 10 cd.s/m² (0 dB) it was 30ms. Following the scotopic recordings, a rod-suppressing background light of 25 cd.s/m² was turned on for 10 minutes. A cone-stimulating light flash was then applied, the light intensity being 10 cd.s/m² (flash duration 79 ms), for photopic ERGs recording. Mixed (rods + cones) ERG measurements were performed simultaneously on both eyes, with flash intensity of 3 cd.s/m², flash duration of 40 ms, and the amplifier set to 0.5 Hz. Five responses were averaged. Amplitudes of a-waves (negative waves) were measured from the baseline to the bottom of the a-wave

trough, and b-wave amplitudes (positive waves) were measured from the bottom of the a-wave trough to the peak of the b-wave. Implicit times of the a- and b- waves were measured from time of stimulus to peaks. Results were expressed in microvolts (μV) for amplitudes and milliseconds (ms) for implicit times. The data obtained from each eye belonging to the same experimental group were averaged.

RT-PCR Inflammation-focused genes array and data analysis

Neural retinas were isolated on ice and directly frozen until RNA isolation. Total RNA was isolated with RNeasy mini kit (Qiagen, Courtaboeuf, Fr) according to the manufacturer's protocols. RNA concentration, purity, and integrity were determined with an Agilent Bio-analyzer. All RNA used had RNA integrity number superior to 8. First-strand cDNA was generated by reverse transcription using 0.7 μg total RNA and the RT2 First Strand Kit (Qiagen). Genomic DNA was removed on RNeasy columns and before reverse transcription according to the manufacturer's protocols. Expression of 84 inflammatory-related genes and 5 housekeeping genes were evaluated in a 96-well plate (including five housekeeping and seven control genes) by the Rat Inflammatory-Autoimmunity RT2 Profiler PCR Array (PARN-077Z, SABiosciences, Qiagen). Gene arrays were processed according to the manufacturer's instructions. Each PCR reaction was performed following manufacturer's instructions, and dissociation curves were performed to control product of amplification. The threshold for calculating cycle threshold (Ct) values was calculated automatically using RQ software (SABiosciences). A fixed threshold was assigned manually, as suggested by the manufacturer. The relative expression of each gene was calculated using the $\Delta\Delta\text{Ct}$ method. Ct values were analyzed with Web-Based PCR Array Data Analysis tools: (<http://www.sabiosciences.com/pcr/arrayanalysis.php>, SABiosciences) to determine the best housekeeping gene (*Rplp1*), the fold change and p value of each gene (t-test Student). Fold changes $\geq \pm 2$ -fold were defined as biologically relevant changes.

***In vivo* ciliary muscle electroporation of a plasmid encoding transferrin in rats**

Plasmids construction

Human Tf cDNA was extracted by NotI digestion from pCMV6-hTf plasmid (Origene, Rockville, USA), and the 2.5kb product was then ligated into a NotI digested pVAX1 fragment (Life

Technologies), downstream of a cytomegalovirus- β promoter, to give pVAX1-Tf. pVAX1 empty was used as a negative control in all experiments. All plasmids were amplified in *Escherichia coli* bacteria and endotoxin-free prepared (EndoFree Plamid Kit; Qiagen, Courtaboeuf, France). Plasmids were diluted in endotoxin-free water containing 77 mM of NaCl (half saline) (saline, NaCl 0.9%, Versol, Laboratoire Aguettant, Lyon, Fr) as previously described (37). The concentration of DNA was determined by spectroscopy measurements (optical density at 260 nm).

In vivo electroporation of the rat ciliary muscle

Wistar adult males rats came from Janvier Laboratory. P23H-line 1 rats (40) were kindly provided by Mathieu Lavail (UCSF, School of Medicine, Beckman Vision Center), breeding at homozygous. Wistar rats (Janvier laboratory) were used as control. Rats were anesthetized as described, before ciliary muscle electrotransfer (ET). Thirty micrograms of plasmid (pVAX1, pVAX1-Tf), in a total volume of 10 μ l, were injected in the ciliary muscle using a 30-gauge disposable needle (BD Micro-Fine syringe, NM Médical, Asnières, Fr) transsclerally posterior to the limbus then electric pulses were delivered as described (37). Adult Wistar rats were sacrificed for ELISA Tf quantification in ocular media and tissues 3 days after ET and for retinal histology analysis 12 days after ET. For light experiment, ET were realized 3 days before light protocol realized as described above, and rats were sacrificed 8 days later. P23H rats were submitted to ET at 4 weeks of age (an age preceding major onset of PR loss in dystrophic rats), and killed at 8 weeks of age. All eyes were managed as described previously for histological analysis. ONL thickness were measured every 500 μ m of each pole the retina and values were averaged. Mean of ONL thickness at superior pole was representative of both poles and represented on figures.

Statistical analysis

Results are presented as mean \pm Standard error on the mean (SEM). Analysis were performed using GraphPad Prism 5 software. Normal distribution of data was checked by the Shapiro–Wilk test. Comparisons between 2 groups were analyzed by unpaired two-tailed Student's *t*-test, and multiples comparisons by one-way ANOVA followed by Bonferroni post-test as appropriate. Non-normally distributed were analysed using nonparametric Kruskal–Wallis test. $p < 0.05$ was considered statistically significant.

Acknowledgements

We thank Dr. Torriglia and Dr. de Kozack (UMRS1138, Centre de Recherche des Cordeliers, INSERM) for their guidance and stimulating discussion. We thank Dr. Reed and Mélanie Glaetli for the english correction and the staff at the animal facility at Centre de Recherche des Cordeliers. The authors wish to thank Paolo Santambrogio (Department Biological and Technological Research, Istituto de Ricovero e Cure a Carattere Scientifico, San Raffaele, Milan, Italy) for rabbit polyclonal specific for the High and Light subunits of Ferritin; John Saari (University of Washington, Seattle, USA) for rabbit anti-cellular retinaldehyde binding protein and Robert S. Molday (University of British Columbia, Vancouver, Canada) for anti-rhodopsin antibody. This study was supported by INSERM, ANR Emergence 2012 (R11086DD), Retina France and Fondation de France-Fondation de l'oeil, Berthe Fouassier.

References

1. Andersen HH, Johnsen KB, and Moos T. Iron deposits in the chronically inflamed central nervous system and contributes to neurodegeneration. *Cell Mol Life Sci.* 2014;71(9):1607-22.
2. Wong RW, Richa DC, Hahn P, Green WR, and Dunaief JL. Iron toxicity as a potential factor in AMD. *Retina.* 2007;27(8):997-1003.
3. Kell DB. Iron behaving badly: inappropriate iron chelation as a major contributor to the aetiology of vascular and other progressive inflammatory and degenerative diseases. *BMC Med Genomics.* 2009;2(2).
4. Moiseyev G, Chen Y, Takahashi Y, Wu BX, and Ma JX. RPE65 is the isomerohydrolase in the retinoid visual cycle. *Proc Natl Acad Sci U S A.* 2005;102(35):12413-8.
5. Shichi H. Microsomal electron transfer system of bovine retinal pigment epithelium. *Exp Eye Res.* 1969;8(1):60-8.
6. Gnana-Prakasam JP, Martin PM, Smith SB, and Ganapathy V. Expression and function of iron-regulatory proteins in retina. *IUBMB Life.* 2010;62(5):363-70.
7. Song D, and Dunaief JL. Retinal iron homeostasis in health and disease. *Front Aging Neurosci.* 2013;5(24).
8. Hahn P, Ying GS, Beard J, and Dunaief JL. Iron levels in human retina: sex difference and increase with age. *Neuroreport.* 2006;17(17):1803-6.
9. Ciudin A, Hernandez C, and Simo R. Iron overload in diabetic retinopathy: a cause or a consequence of impaired mechanisms? *Exp Diabetes Res.* 2010;2010(
10. Hahn P, Milam AH, and Dunaief JL. Maculas affected by age-related macular degeneration contain increased chelatable iron in the retinal pigment epithelium and Bruch's membrane. *Arch Ophthalmol.* 2003;121(8):1099-105.
11. Junemann AG, Stopa P, Michalke B, Chaudhri A, Reulbach U, Huchzermeyer C, Schlotzer-Schrehardt U, Kruse FE, Zrenner E, and Rejdak R. Levels of aqueous humor trace elements in patients with non-exsudative age-related macular degeneration: a case-control study. *PLoS One.* 2013;8(2):e56734.
12. Rogers BS, Symons RC, Komeima K, Shen J, Xiao W, Swaim ME, Gong YY, Kachi S, and Campochiaro PA. Differential sensitivity of cones to iron-mediated oxidative damage. *Invest Ophthalmol Vis Sci.* 2007;48(1):438-45.
13. Yefimova MG, Jeanny JC, Keller N, Sergeant C, Guillonneau X, Beaumont C, and Courtois Y. Impaired retinal iron homeostasis associated with defective phagocytosis in Royal College of Surgeons rats. *Invest Ophthalmol Vis Sci.* 2002;43(2):537-45.
14. Picard E, Jonet L, Sergeant C, Vesvres MH, Behar-Cohen F, Courtois Y, and Jeanny JC. Overexpressed or intraperitoneally injected human transferrin prevents photoreceptor degeneration in rd10 mice. *Mol Vis.* 2010;16(26):12-25.
15. Deleon E, Lederman M, Berenstein E, Meir T, Chevion M, and Chowers I. Alteration in iron metabolism during retinal degeneration in rd10 mouse. *Invest Ophthalmol Vis Sci.* 2009;50(3):1360-5.
16. Boddaert N, Le Quan Sang KH, Rotig A, Leroy-Willig A, Gallet S, Brunelle F, Sidi D, Thalabard JC, Munnich A, and Cabantchik ZI. Selective iron chelation in Friedreich ataxia: biologic and clinical implications. *Blood.* 2007;110(1):401-8.
17. Devos D, Moreau C, Devedjian JC, Kluza J, Petrault M, Laloux C, Jonneaux A, Ryckewaert G, Garcon G, Rouaix N, et al. Targeting chelatable iron as a therapeutic modality in Parkinson's disease. *Antioxid Redox Signal.* 2014;21(2):195-210.
18. Hadziahmetovic M, Pajic M, Grieco S, Song Y, Song D, Li Y, Cwanger A, Iacovelli J, Chu S, Ying GS, et al. The Oral Iron Chelator Deferiprone Protects Against Retinal Degeneration Induced through Diverse Mechanisms. *Transl Vis Sci Technol.* 2012;1(3):2.
19. Hadziahmetovic M, Pajic M, Grieco S, Song Y, Song D, Li Y, Cwanger A, Iacovelli J, Chu S, Ying GS, et al. The Oral Iron Chelator Deferiprone Protects Against Retinal Degeneration Induced through Diverse Mechanisms. *Transl Vis Sci Technol.* 2012;1(2):7.

20. Hadziahmetovic M, Song Y, Wolkow N, Iacovelli J, Grieco S, Lee J, Lyubarsky A, Pratico D, Connelly J, Spino M, et al. The oral iron chelator deferiprone protects against iron overload-induced retinal degeneration. *Invest Ophthalmol Vis Sci.* 2011;52(2):959-68.
21. Obolensky A, Berenshtein E, Lederman M, Bulvik B, Alper-Pinus R, Yaul R, Deleon E, Chowers I, Chevion M, and Banin E. Zinc-desferrioxamine attenuates retinal degeneration in the rd10 mouse model of retinitis pigmentosa. *Free Radic Biol Med.* 2011;51(8):1482-91.
22. Baath JS, Lam WC, Kirby M, and Chun A. Deferoxamine-related ocular toxicity: incidence and outcome in a pediatric population. *Retina.* 2008;28(6):894-9.
23. Wong A, Alder V, Robertson D, Papadimitriou J, Maserei J, Berdoukas V, Kontoghiorghes G, Taylor E, and Baker E. Liver iron depletion and toxicity of the iron chelator deferiprone (L1, CP20) in the guinea pig. *Biometals.* 1997;10(4):247-56.
24. Picard E, Fontaine I, Jonet L, Guillou F, Behar-Cohen F, Courtois Y, and Jeanny JC. The protective role of transferrin in Muller glial cells after iron-induced toxicity. *Mol Vis.* 2008;14(9):28-41.
25. Picard E, Ranchon-Cole I, Jonet L, Beaumont C, Behar-Cohen F, Courtois Y, and Jeanny JC. Light-induced retinal degeneration correlates with changes in iron metabolism gene expression, ferritin level, and aging. *Invest Ophthalmol Vis Sci.* 2011;52(3):1261-74.
26. Yefimova MG, Jeanny JC, Guillonneau X, Keller N, Nguyen-Legros J, Sergeant C, Guillou F, and Courtois Y. Iron, ferritin, transferrin, and transferrin receptor in the adult rat retina. *Invest Ophthalmol Vis Sci.* 2000;41(8):2343-51.
27. Noell WK, Walker VS, Kang BS, and Berman S. Retinal damage by light in rats. *Invest Ophthalmol.* 1966;5(5):450-73.
28. Marc RE, Jones BW, Watt CB, Vazquez-Chona F, Vaughan DK, and Organisciak DT. Extreme retinal remodeling triggered by light damage: implications for age related macular degeneration. *Mol Vis.* 2008;14(7):82-806.
29. Martin PM, Gnana-Prakasam JP, Roon P, Smith RG, Smith SB, and Ganapathy V. Expression and polarized localization of the hemochromatosis gene product HFE in retinal pigment epithelium. *Invest Ophthalmol Vis Sci.* 2006;47(10):4238-44.
30. Margrain TH, Boulton M, Marshall J, and Sliney DH. Do blue light filters confer protection against age-related macular degeneration? *Prog Retin Eye Res.* 2004;23(5):523-31.
31. Wielgus AR, Collier RJ, Martin E, Lih FB, Tomer KB, Chignell CF, and Roberts JE. Blue light induced A2E oxidation in rat eyes--experimental animal model of dry AMD. *Photochem Photobiol Sci.* 2010;9(11):1505-12.
32. Hadziahmetovic M, Kumar U, Song Y, Grieco S, Song D, Li Y, Tobias JW, and Dunaief JL. Microarray analysis of murine retinal light damage reveals changes in iron regulatory, complement, and antioxidant genes in the neurosensory retina and isolated RPE. *Invest Ophthalmol Vis Sci.* 2012;53(9):5231-41.
33. Hentze MW, Muckenthaler MU, Galy B, and Camaschella C. Two to tango: regulation of Mammalian iron metabolism. *Cell.* 2010;142(1):24-38.
34. Rutar M, Provis JM, and Valter K. Brief exposure to damaging light causes focal recruitment of macrophages, and long-term destabilization of photoreceptors in the albino rat retina. *Curr Eye Res.* 2010;35(7):631-43.
35. Santos AM, Martin-Oliva D, Ferrer-Martin RM, Tassi M, Calvente R, Sierra A, Carrasco MC, Marin-Teva JL, Navascues J, and Cuadros MA. Microglial response to light-induced photoreceptor degeneration in the mouse retina. *J Comp Neurol.* 2010;518(4):477-92.
36. Organisciak DT, and Vaughan DK. Retinal light damage: mechanisms and protection. *Prog Retin Eye Res.* 2010;29(2):113-34.
37. Touchard E, Kowalczyk L, Bloquel C, Naud MC, Bigey P, and Behar-Cohen F. The ciliary smooth muscle electrotransfer: basic principles and potential for sustained intraocular production of therapeutic proteins. *J Gene Med.* 2010;12(11):904-19.

38. Touchard E, Bloquel C, Bigey P, Kowalczyk L, Jonet L, Thillaye-Goldenberg B, Naud MC, Scherman D, de Kozak Y, Benezra D, et al. Effects of ciliary muscle plasmid electrotransfer of TNF-alpha soluble receptor variants in experimental uveitis. *Gene Ther.* 2009;16(7):862-73.
39. Touchard E, Heiduschka P, Berdugo M, Kowalczyk L, Bigey P, Chahory S, Gandolphe C, Jeanny JC, and Behar-Cohen F. Non-viral gene therapy for GDNF production in RCS rat: the crucial role of the plasmid dose. *Gene Ther.* 2012;19(9):886-98.
40. Lee D, Geller S, Walsh N, Valter K, Yasumura D, Matthes M, LaVail M, and Stone J. Photoreceptor degeneration in Pro23His and S334ter transgenic rats. *Adv Exp Med Biol.* 2003;533(297-302).
41. Hadziahmetovic M, Song Y, Wolkow N, Iacovelli J, Kautz L, Roth MP, and Dunaief JL. Bmp6 regulates retinal iron homeostasis and has altered expression in age-related macular degeneration. *Am J Pathol.* 2011;179(1):335-48.
42. Forni GL, Balocco M, Cremonesi L, Abbruzzese G, Parodi RC, and Marchese R. Regression of symptoms after selective iron chelation therapy in a case of neurodegeneration with brain iron accumulation. *Mov Disord.* 2008;23(6):904-7.
43. Finkenstedt A, Wolf E, Hofner E, Gasser BI, Bosch S, Bakry R, Creus M, Kremser C, Schocke M, Theurl M, et al. Hepatic but not brain iron is rapidly chelated by deferasirox in aceruloplasminemia due to a novel gene mutation. *J Hepatol.* 2010;53(6):1101-7.
44. Abbruzzese G, Cossu G, Balocco M, Marchese R, Murgia D, Melis M, Galanello R, Barella S, Matta G, Ruffinengo U, et al. A pilot trial of deferiprone for neurodegeneration with brain iron accumulation. *Haematologica.* 2011;96(11):1708-11.
45. Pratini NR, Sweeters N, Vichinsky E, and Neufeld JA. Treatment of classic pantothenate kinase-associated neurodegeneration with deferiprone and intrathecal baclofen. *Am J Phys Med Rehabil.* 2013;92(8):728-33.
46. Song D, Song Y, Hadziahmetovic M, Zhong Y, and Dunaief JL. Systemic administration of the iron chelator deferiprone protects against light-induced photoreceptor degeneration in the mouse retina. *Free Radic Biol Med.* 2012;53(1):64-71.
47. Song D, Zhao L, Li Y, Hadziahmetovic M, Song Y, Connelly J, Spino M, and Dunaief JL. The oral iron chelator deferiprone protects against systemic iron overload-induced retinal degeneration in hepcidin knockout mice. *Invest Ophthalmol Vis Sci.* 2014;55(7):4525-32.
48. Rahi AH, Hungerford JL, and Ahmed AI. Ocular toxicity of desferrioxamine: light microscopic histochemical and ultrastructural findings. *Br J Ophthalmol.* 1986;70(5):373-81.
49. Cases A, Kelly J, Sabater J, Campistol JM, Torras A, Montoliu J, Lopez I, and Revert L. Acute visual and auditory neurotoxicity in patients with end-stage renal disease receiving desferrioxamine. *Clin Nephrol.* 1988;29(4):176-8.
50. Kontoghiorghes GJ. Deferasirox: uncertain future following renal failure fatalities, agranulocytosis and other toxicities. *Expert Opin Drug Saf.* 2007;6(3):235-9.
51. Nemeth E, Tuttle MS, Powelson J, Vaughn MB, Donovan A, Ward DM, Ganz T, and Kaplan J. Hepcidin regulates cellular iron efflux by binding to ferroportin and inducing its internalization. *Science.* 2004;306(5704):2090-3.
52. Gnana-Prakasam JP, Martin PM, Mysona BA, Roon P, Smith SB, and Ganapathy V. Hepcidin expression in mouse retina and its regulation via lipopolysaccharide/Toll-like receptor-4 pathway independent of Hfe. *Biochem J.* 2008;411(1):79-88.
53. Schmidt PJ, Toran PT, Giannetti AM, Bjorkman PJ, and Andrews NC. The transferrin receptor modulates Hfe-dependent regulation of hepcidin expression. *Cell Metab.* 2008;7(3):205-14.
54. Ruchala P, and Nemeth E. The pathophysiology and pharmacology of hepcidin. *Trends Pharmacol Sci.* 2014;35(3):155-61.
55. Hadziahmetovic M, Song Y, Ponnuru P, Iacovelli J, Hunter A, Haddad N, Beard J, Connor JR, Vaulont S, and Dunaief JL. Age-dependent retinal iron accumulation and degeneration in hepcidin knockout mice. *Invest Ophthalmol Vis Sci.* 2011;52(1):109-18.

56. Fleming RE, Migas MC, Holden CC, Waheed A, Britton RS, Tomatsu S, Bacon BR, and Sly WS. Transferrin receptor 2: continued expression in mouse liver in the face of iron overload and in hereditary hemochromatosis. *Proc Natl Acad Sci U S A*. 2000;97(5):2214-9.
57. Wysokinski D, Blasiak J, Dorecka M, Kowalska M, Robaszekiewicz J, Pawlowska E, Szaflik J, and Szaflik JP. Variability of the transferrin receptor 2 gene in AMD. *Dis Markers*. 2014;2014(507356).
58. Kim TH, Zhao Y, Barber MJ, Kuharsky DK, and Yin XM. Bid-induced cytochrome c release is mediated by a pathway independent of mitochondrial permeability transition pore and Bax. *J Biol Chem*. 2000;275(50):39474-81.
59. Fassl S, Leisser C, Huettenbrenner S, Maier S, Rosenberger G, Strasser S, Grusch M, Fuhrmann G, Leuhuber K, Polgar D, et al. Transferrin ensures survival of ovarian carcinoma cells when apoptosis is induced by TNFalpha, FasL, TRAIL, or Myc. *Oncogene*. 2003;22(51):8343-55.
60. Lesnikov V, Gordien N, Fausto N, Spaulding E, Campbell J, Shulman H, Fleming RE, and Deeg HJ. Transferrin fails to provide protection against Fas-induced hepatic injury in mice with deletion of functional transferrin-receptor type 2. *Apoptosis*. 2008;13(8):1005-12.
61. Mangano K, Fagone P, Di Mauro M, Ascione E, Maiello V, Milicic T, Jotic A, Lalic NM, Saksida T, Stojanovic I, et al. The immunobiology of apotransferrin in type 1 diabetes. *Clin Exp Immunol*. 2012;169(3):244-52.
62. Saksida T, Miljkovic D, Timotijevic G, Stojanovic I, Mijatovic S, Fagone P, Mangano K, Mammanna S, Farina C, Ascione E, et al. Apotransferrin inhibits interleukin-2 expression and protects mice from experimental autoimmune encephalomyelitis. *J Neuroimmunol*. 2013;262(1-2):72-8.
63. Pierpaoli W, Bulian D, and Arrighi S. Transferrin treatment corrects aging-related immunologic and hormonal decay in old mice. *Exp Gerontol*. 2000;35(3):401-8.
64. McGahan MC, Grimes AM, and Fleisher LN. Transferrin inhibits the ocular inflammatory response. *Exp Eye Res*. 1994;58(4):509-11.
65. Rutar M, Natoli R, Valter K, and Provis JM. Early focal expression of the chemokine Ccl2 by Muller cells during exposure to damage-inducing bright continuous light. *Invest Ophthalmol Vis Sci*. 2011;52(5):2379-88.
66. Sennlaub F, Auvynet C, Calippe B, Lavalette S, Poupel L, Hu SJ, Dominguez E, Camelo S, Levy O, Guyon E, et al. CCR2(+) monocytes infiltrate atrophic lesions in age-related macular disease and mediate photoreceptor degeneration in experimental subretinal inflammation in Cx3cr1 deficient mice. *EMBO Mol Med*. 2013;5(11):1775-93.
67. Joly S, Francke M, Ulbricht E, Beck S, Seeliger M, Hirrlinger P, Hirrlinger J, Lang KS, Zinkernagel M, Odermatt B, et al. Cooperative phagocytes: resident microglia and bone marrow immigrants remove dead photoreceptors in retinal lesions. *Am J Pathol*. 2009;174(6):2310-23.
68. Milatovic D, Zaja-Milatovic S, Montine KS, Shie FS, and Montine TJ. Neuronal oxidative damage and dendritic degeneration following activation of CD14-dependent innate immune response in vivo. *J Neuroinflammation*. 2004;1(1):20.
69. Ni YQ, Xu GZ, Hu WZ, Shi L, Qin YW, and Da CD. Neuroprotective effects of naloxone against light-induced photoreceptor degeneration through inhibiting retinal microglial activation. *Invest Ophthalmol Vis Sci*. 2008;49(6):2589-98.
70. Yang D, Elnor SG, Lin LR, Reddy VN, Petty HR, and Elnor VM. Association of superoxide anions with retinal pigment epithelial cell apoptosis induced by mononuclear phagocytes. *Invest Ophthalmol Vis Sci*. 2009;50(10):4998-5005.
71. Lin T, Walker GB, Kurji K, Fang E, Law G, Prasad SS, Kojic L, Cao S, White V, Cui JZ, et al. Parainflammation associated with advanced glycation endproduct stimulation of RPE in vitro: implications for age-related degenerative diseases of the eye. *Cytokine*. 2013;62(3):369-81.
72. Laye S, Liege S, Li KS, Moze E, and Neveu PJ. Physiological significance of the interleukin 1 receptor accessory protein. *Neuroimmunomodulation*. 2001;9(4):225-30.

73. Ali S, Huber M, Kollewe C, Bischoff SC, Falk W, and Martin MU. IL-1 receptor accessory protein is essential for IL-33-induced activation of T lymphocytes and mast cells. *Proc Natl Acad Sci U S A*. 2007;104(47):18660-5.
74. De Vera Mudry MC, Kronenberg S, Komatsu S, and Aguirre GD. Blinded by the light: retinal phototoxicity in the context of safety studies. *Toxicol Pathol*. 2013;41(6):813-25.

LEGENDS

Figure 1: Time-related distribution of transferrin after intravitreal injection in normal rats.

(A-E) Adult Wistar rat received one intravitreal injection of transferrin (Tf) labeled with fluorochrom Alexa 488 (green). (A) Two hours after injection, Tf-Alexa 488 (left) co-localized (right) with Müller glial cells stained with anti-cellular retinaldehyde-binding protein (CRALBP) antibody (middle). (B-C) Higher magnification revealed Tf-Alexa on apical side of retinal pigment epithelium revealed with anti-RPE65 antibody (red) (B), and at photoreceptors segments layers stained with rhodopsin (red, asterisk) (C). (D) Tf-Alexa merged (yellow) with transferrin receptor 1 (red) in synaptic layers. (E) Tf-Alexa co-localized with transferrin receptor 2 (red) in inner segments, outer nuclear layer and inner plexiform layer. (F) Six hours after injection, Tf-Alexa was in overall retina and additionally detected in choroid (Ch) vessels. (G-H) Transferrin levels were quantified in posterior segment tissues (G) and ocular fluids (H) by ELISA assay, 6 and 24 hours after Tf injection. All values are represented as mean \pm SEM. Student's t-test; n=3-4 rats per time; ** p=0.0032; *** p<0.0001.

Ch: Choroid; GCL: Ganglion cell layer; INL: Inner nuclear layer; IPL: Inner plexiform layer; IS: Inner segment; ONL: Outer nuclear layer; OPL: Outer plexiform layer; OS: Outer segment; RPE: retinal pigment epithelium. Scale bars A, C, D-F: 50 μ m; B: 20 μ m. Nuclei stained with DAPI (blue).

Figure 2: IVT injections of transferrin have no retinal toxicity.

(A) *In vivo* retinal structure recorded by optical coherence tomography (OCT) 7 days after first transferrin (Tf) IVT injection (D7) and 7 days after the second Tf injection (D14) in rats, demonstrated no retinal histological modifications. (B) Measurement of outer nuclear layer (ONL) from OCT pictures in control not injected rats and rats injected once (D7) or twice (D14) with Tf. (C) Pictures of

historesin semi-thin sagittal retinal sections 7 days after the second Tf injection. **(D)** Mean ONL thickness measured on sections crossing the optic nerve in overall retina of control rats and twice Tf-injected rats.

All values are represented as mean \pm SEM; Student's t-test; n=4 eyes per group; ns= not significant.

GCL: Ganglion cell layer; INL: Inner nuclear layer; IPL: Inner plexiform layer; IS: Inner segment; ONL: Outer nuclear layer; OPL: Outer plexiform layer; OS: Outer segment; RPE: retinal pigment epithelium. Scale bar A: 200 μ m; C: 100 μ m.

Figure 3: Intravitreal injection of transferrin protects rat retina against light-induced retinal degeneration.

Transferrin (Tf) was injected in rats before a 24-hours continuous light exposure, analyses were performed after 8 days. **(A)** *In vivo* optical coherence tomography (OCT) images showed a reduction of outer nuclear layer (ONL) thickness in BLE rats compare to NLE and TfLE rats. **(B)** ONL thickness of superior pole (500 to 3,000 μ m from optic nerve) measured on OCT pictures in intervals of 500 μ m, in NLE, BLE and TfLE rats. **(C)** Retinal semi-thin sections at the superior pole showed important photoreceptor nuclei layer (ONL) degeneration in BLE rats as compared to control (NLE) or TfLE rats. **(D)** Measures of ONL thickness, with intervals of 500 μ m, across the entire retina show that Tf-treatment significantly protect photoreceptors nuclei layer thickness as compared to BSS treatment.

BLE: Rats injected with BSS and exposed to light (red lines); NLE: Control rats neither injected nor exposed to light (black lines); TfLE: Rats injected with human Tf and exposed to light (blue lines). All values are represented as mean \pm SEM; One-way ANOVA, followed with Bonferroni post-test. n=8-10 eyes per group; significant differences (***) p <0.001) were observed between TfLE and BLE. All statistic analyses can be found in Supp. Table 1. GCL: Ganglion cell layer; INL: Inner nuclear layer; IS: Inner segment; ONL: Outer nuclear layer; OS: Outer segment; RPE: retinal pigment epithelium. Scale bars: A: 200 μ m, C: 100 μ m.

Figure 4: Transferrin decreases light-induced photoreceptors apoptosis and preserves visual activities.

(A) TUNEL staining (red) and (B) fluorescence intensity quantification at the photoreceptors nuclei layer, 1 day after light exposure show a reduction of apoptosis in TfLE compared to BLE retinas. Mann-Whitney test; n=3-4 retinas per group; *p=0.0201. (C) Rods immunostaining (green, top panel) and cones lectin staining (green, bottom panel, arrows) in rats at 8 days reflect the integrity of TfLE photoreceptors. (D) Scotopic electroretinogram, specific to rod-driven responses, was recorded 16 days after light exposure. Light (red lines) induced a collapse of a-waves (dotted lines) and b-waves (solid waves) amplitudes. Those amplitudes were preserved in TfLE (blue lines) and reached nearly 50% of NLE values (black lines). One-way ANOVA, followed with Bonferroni post-test. n=8 eyes per group; significant differences (*p<0.05, **p<0.01) were observed between TfLE and BLE. (E) Photopic ERG was recorded after saturation of rods to obtain specific cone response. The amplitude (left part) and the implicit time (right part) of the b-wave are represented on the graph. While the light induced reduction of the b-wave amplitude was not prevented by the injection of Tf (blue bar), the treatment normalized the b-wave implicit time (shaded blue bar). One-way ANOVA, followed with Bonferroni post-test. n=8 eyes per group; significant differences (*p<0.05, **p<0.01). (F) Quantification of cones on superior pole. BLE group and TfLE are expressed relative to the control group (NLE). Percentage of cones reduced in BLE rats was partially preserved in TfLE rats. Mann-Whitney t-test; n= 3 eyes per group; * p<0.05.

BLE: Rats injected with BSS and exposed to light (red); NLE: Control rats neither exposed to light, neither injected (black); TfLE: Rats injected with human Tf and exposed to light (blue). All values are represented as mean \pm SEM. (Complete statistic analysis for D and E can be found in Supp. Table 1. INL: Inner nuclear layer; ONL: Outer nuclear layer. A, C: Nuclei stained with DAPI. Scale bars A: 100 μ m; C: 20 μ m.

Figure 5: Transferrin treatment controls iron metabolism.

(A) Quantitative PCR of iron-related genes mRNA normalized with Ribosomal Protein P1 (*Rplp1*) mRNA on neural retina one day after light exposure. Transcripts related to transport (*Tf* and *TfR1*),

storage (Ferritin Heavy chain (*FtH*) and Light chain (*FtL*)), export (Divalent metal transporter 1 (*Dmt1*), Ferroportin (*Fpn*), Ceruloplasmin (*Cp*)) and regulation of iron (*TfR2*, Human hemochromatosis protein (*Hfe*), Hemojuvelin (*Hjuv*)) were modified following light exposure when comparing BLE to NLE rats. When comparing TfLE to BLE retinas, Tf-treatment modulated the expression of several of these iron-related mRNAs. All values are represented as mean \pm SEM; One-way ANOVA, Bonferroni post-test; n=5-6 neural retinas; * p<0.05; ** p<0.01; *** p<0.001, ns= not significant. **(B-D)** Immunohistochemistry of ferritins and transferrin receptor 1 on retinal sections 3 days after light exposure. Heavy chain (B) and light chain (C) ferritins and transferrin receptor 1 staining (D) were conserved in TfLE rat retinas (right column) as compared to NLE rat retinas (left column), whereas proteins staining intensities were modified in BLE rat retinas (central column). Nuclei stained with DAPI (blue). Scale bar B-D: 100 μ m. **(E)** Iron labeling on retinal cryosections demonstrate iron accumulation in outer retinas of BLE rats at 8 days after light exposure. TfLE retinas iron staining was similar to NLE rat retinas. Scale bar: 100 μ m. **(F)** Total non-heme iron quantification in the retinas demonstrate that Tf prevented free iron content to increase after light exposure. All values are represented as mean \pm SEM; Kruskal-Wallis, Dunn post-test; n=3-4 retinas; * p<0.05. BLE: Rats injected with BSS and exposed to light (red); NLE: Control rats neither injected nor exposed to light (black); TfLE: Rats injected with human Tf and exposed to light (blue).

Figure 6: Transferrin inhibits light-induced oxidative stress.

Heme oxygenase 1 (*Hmox1*) mRNA expression related to control gene Ribosomal Protein P1 (*Rplp1*) was determined in neural retina one day after light-injury. While light exposure drastically increases *Hmox1* gene expression (BLE group), Tf injection significantly reduced this increase (TfLE group). All values are represented as mean of fold change \pm SEM. One-way ANOVA, Bonferroni post-test; n=5-6 retina per group; *p<0.05; *** p<0.001; ns = not significant. BLE: Rats injected with BSS and exposed to light (red bar); NLE: Control rats neither injected nor exposed to light (black bar); TfLE: Rats injected with human Tf and exposed to light (blue bar).

Figure 7: Transferrin injection manages inflammatory cells responses.

(A) In control group, microglia cells (arrow) anti-ionized calcium binding adaptor molecule 1 (Iba1) positive were localized in inner retina and negative for anti-CD68, marker of activation. (B-G) Microglial/macrophages cells migrated in photoreceptors layer (arrows) after light-exposure as observed 1 (B-C), 3 (D-E) or 8 (G-H) days after light period. (D2-E2) Higher magnification of corresponding area delimited in outer retina of D and E revealed more Iba1+/CD68+ co-staining in BLE rats than in TfLE rats. (F) Quantification of CD68 positive cells staining were reported to Iba1 cells intensity staining measured in outer retina 3 days after light period. Microglial/macrophages activation after light exposure was reduced with Tf injection. All values are represented as mean± SEM. Mann-Whitney test; n=3 eyes per time; *p=0.0104. (G-H) At day 8, in BLE rat retinas, microglial/macrophages cells accumulated in outer retina (arrows, G) compared to TfLE retinas (arrowheads, H).

Rats injected with BSS and exposed to light (red bar); TfLE: Rats injected with human Tf and exposed to light (blue bar). Scale bar A-H: 100µm; D2-E2: 50µm.

Figure 8. Volcano plots of mRNAs regulated by transferrin in light exposed retinas.

Volcano plot of 84 differentially expressed genes in light exposed retinas treated with Tf relative to control treatment ($n = 5-6$ per group) according to their p-value versus fold change. Highest fold change expression ($|\text{Log}_2^{\text{(fold change)}}| \geq 2$) are colored. Significant differences were determined with Student's t-test ($p < 0.05$; $n = 5-6$ retinas per group). BLE: Rats injected with BSS and exposed to light (red bar); TfLE: Rats injected with human Tf and exposed to light (blue bar).

Figure 9: Intravitreal injection of transferrin partially protects degenerated retina.

After a dark adaptation period, rats were placed under a 24-hour intense light treatment. We subsequently injected Tf or BSS solutions via IVT, and sacrificed them 8 days later. (A) Historesin blue-stained sections on inferior pole demonstrate partial preservation of retina structure with Tf injection. ONL: Outer nuclear layer. Scale bar: 100µm. (B) ONL thickness measurement throughout the retina, every 500µm, showed protective effect of Tf only in the inferior pole. All values are

represented as mean \pm SEM; TfLE retinas were compared to BLE at each different distance from the optic nerve with one-way ANOVA, Bonferroni post-test; n=8 eyes per group; *** p<0.001. BLE: Rats injected with BSS and exposed to light (red line); NLE: Control rats neither injected nor exposed to light (black line); TfLE: Rats injected with human Tf and exposed to light (blue line).

Figure 10: Non-viral gene therapy for local transferrin production preserves photoreceptors in 2 models of retinal degeneration.

(A) Histology of the retina following electrotransfer of empty plasmid (pVAX1) or containing cDNA of transferrin (pVAX1-Tf). (B) Mean ONL thickness evaluated on histoiresin semi-thin retinal sections in control rats (black bar), and 12 days after ET of pVAX1 (red bar) or pVAX1-Tf (blue bar) in rats. ET and substained production of Tf had no deleterious effect on retina structure. (C) Histoiresin sections (D) and mean of ONL thickness of rats electrotransferred with pVAX1 (red bar) or pVAX-Tf (blue bar), submitted to light-exposure (LE) 3 days after, and sacrificed 8 days later. Control rats not ET but exposed to light are represented with black bar (control, LE). (E) Histoiresin sections and mean of ONL thickness (F) of P23H rats retinas (black bar), model of slow retinal degeneration, electrotransferred at 4 weeks of age with pVAX1 (red bar) or pVAX-Tf plasmids (blue bar), and sacrificed 4 weeks later. Scale bar: 100 μ m; All values are represented as mean \pm SEM; One-way ANOVA, Bonferroni post-test; n=6-10 eyes per group; *p<0.05; *** p<0.001; ns=not significant.

Figure 11: Treatments with transferrin remove retinal iron deposits in a mouse model of iron overload.

(A) Iron staining (blue) by Perls method in the RPE of 32 weeks-old mice *Bmp6*^{-/-} (control), intraperitoneally (IP) injected with BSS or Tf. Sections were counterstained with nuclear red. RPE: Retinal pigment epithelium. Scale bar: 10 μ m. (B) Quantification of iron staining in retinal pigment epithelium (RPE) in 32 weeks-old *Bmp6* KO mice (black bar), treated with Tf (blue bar) or BSS (red bar) by IP injections, 3 times per week for one month, or with a single intravitreal injection. All values are represented as mean \pm SEM; Student's t-test; n=4-6 retinas per group; *p=0.0475; **p=0.0035

Table 1

Gene	Refseq	BLE / NLE	p value	TfLE / NLE	p value
Cytokines					
Chemokines					
<i>Ccl2</i>	NM_031530	19,50	0,0067	23,19	0,0278
<i>Ccl3</i>	NM_013025	1,67	0,1277	2,01	0,0977
<i>Ccl4</i>	NM_053858	1,36	0,6613	1,83	0,355
<i>Ccl5</i>	NM_031116	-2,27	0,0642	-1,09	0,5834
<i>Ccl6</i>	NM_001004202	1,16	0,4972	3,57	0,0241
<i>Ccl7</i>	NM_001007612	141,29	0,0084	139,54	0,0669
<i>Ccl12</i>	NM_001105822	39,93	0,021	33,79	0,0012
<i>Ccl20</i>	NM_019233	1,33	0,6313	2,58	0,1097
<i>Ccl21</i>	NM_001008513	-2,25	0,0956	-1,48	0,8691
<i>Ccl22</i>	NM_057203	-1,22	0,5055	2,26	0,3109
<i>Ccl24</i>	NM_001013045	-3,01	0,0994	-1,80	0,0031
<i>Cxcl1</i>	NM_030845	3,31	0,0049	3,54	0,0742
<i>Cxcl3</i>	NM_138522	4,10	0,0048	8,77	2,2E-05
<i>Cxcl5</i>	NM_022214	-1,02	0,9667	2,43	0,1864
<i>Cxcl9</i>	NM_145672	4,76	0,0126	13,72	0,0314
<i>Cxcl10</i>	NM_139089	4,64	0,0395	4,44	0,0947
<i>Cxcl11</i>	NM_182952	4,24	0,0032	3,85	0,0001
Interleukins					
<i>Il1a</i>	NM_017019	11,67	0,1829	16,80	0,0426
<i>Il1b</i>	NM_031512	1,79	0,357	7,73	0,0593
<i>Il5</i>	NM_021834	-9,09	0,0515	-3,33	0,1385
<i>Il6</i>	NM_012589	3,83	0,4927	6,02	0,1943
<i>Il7</i>	NM_013110	-1,62	0,2695	-2,23	0,1356
<i>Il9</i>	NM_001105747	-1,05	0,881	3,61	0,0695
<i>Il10</i>	NM_012854	-1,65	0,1272	-2,04	0,0637
<i>Il17a</i>	NM_001106897	-3,29	0,1357	-1,75	0,3971
<i>Il18</i>	NM_019165	1,98	0,0103	2,52	0,0006
<i>Il22</i>	XM_576228	-1,65	0,2752	-2,93	0,1197
<i>Il23a</i>	NM_130410	-2,17	0,0385	-2,11	0,0317
Others inflammatory molecules					
<i>Cd401g</i>	NM_053353	3,90	0,7813	2,68	0,8795
<i>Crp</i>	NM_017096	-3,42	0,0818	-2,82	0,0687
<i>Csf1</i>	NM_023981	3,39	0,0008	2,60	0,037
<i>Faslg</i>	NM_012908	-1,75	0,0865	-2,94	0,0198
<i>Ifng</i>	NM_138880	2,20	0,3781	-1,89	0,5869
<i>Kng1</i>	NM_012696	-1,40	0,1172	-1,64	0,0822
<i>Lta</i>	NM_080769	-2,35	0,0972	-1,48	0,5197
<i>Tnf</i>	NM_212507	2,71	0,7748	2,48	0,7756
<i>Tnfsf14</i>	XM_236794	9,88	0,0477	12,89	0,0604
Cytokines Receptors					
<i>Ccr1</i>	NM_020542	9,34	0,1125	17,14	0,1241
<i>Ccr2</i>	NM_021866	20,61	0,1823	23,51	0,1025
<i>Ccr3</i>	NM_053958	-2,61	0,2377	2,98	0,2298
<i>Ccr4</i>	NM_133532	6,57	0,1385	8,53	0,0147
<i>Cxcr2</i>	NM_017183	4,58	0,3733	18,44	0,2491
<i>Cd14</i>	NM_021744	18,41	0,0422	23,18	0,008
<i>Il1r1</i>	NM_013123	2,46	0,0073	2,34	0,0077
<i>Il1rap</i>	NM_012968	1,25	0,6099	-1,37	0,2529
<i>Il1rn</i>	NM_022194	4,84	0,2192	13,73	0,0729
<i>Il8ra</i>	NM_019310	1,07	0,8021	2,11	0,2735
<i>Il23r</i>	XM_001072576	2,70	0,0284	1,19	0,5756
Regulation of Inflammatory Response					
<i>B2m</i>	NM_012512	3,05	1,6E-06	3,48	1,2E-05
<i>C3</i>	NM_016994	2,27	0,1503	2,30	0,0478
<i>C3ar1</i>	NM_032060	3,15	0,0933	4,23	0,0036
<i>Cebpb</i>	NM_024125	3,25	0,013	2,32	0,0351
<i>Itgb2</i>	NM_001037780	3,12	0,0615	5,46	0,0038
<i>Sele</i>	NM_138879	2,41	0,0433	2,33	0,0979
<i>Nos2</i>	NM_012611	-2,43	0,0476	-1,95	0,1874
<i>Nr3c1</i>	NM_012576	-2,48	0,0354	-2,58	0,0294
<i>Tirap</i>	XM_001055833	-2,28	0,0782	-2,23	0,0819
<i>Tollip</i>	NM_001109668	-2,76	0,0443	-1,79	0,0866

<i>Tlr1</i>	NM_001172120	5,26	0,063	8,11	0,0103
<i>Tlr2</i>	NM_198769	3,68	0,0904	5,41	0,0054
<i>Tlr3</i>	NM_198791	3,36	0,0414	3,00	0,067
<i>Tlr5</i>	NM_001145828	6,35	0,2831	2,49	0,4212
<i>Tlr7</i>	NM_001097582	2,67	0,0582	2,27	0,0535

Table1: Inflammatory genes name, RefSeq, functional grouping, and fold change with p value in neural retinas one day after light exposure.

Results are presented as the average fold change in gene expression obtained in rats injected with BSS and exposed to light (BLE) compared to unexposed rats (BLE/NLE), and in rats injected with transferrin and exposed to light (TfLE) rats compared to NLE rats (TfLE/NLE). Transcripts up-regulated (blue) and down-regulated (red) more than 2-fold were represented. Significant differences determined with Student's t-test ($p < 0.05$; $n = 5-6$ retinas per group) were bold.

Analysis	Figures	Parameters measured	Groups			Statistic comparisons			
			NLE	BLE	TfLE	NLE vs BLE	NLE vs TfLE	TfLE vs BLE	
OCT	3B	ONL thickness at superior pole	63.33 μm ± 0.43	35.52 μm ± 3.35	65.13 μm ± 0.85	***	ns	***	
Histology	3D	ONL thickness at superior pole	41.64 μm ± 1.77	8.96 μm ± 1.20	29.31 μm ± 1.68	***	***	***	
	3D	ONL thickness at inferior pole	39.3 μm ± 1.55	23.25 μm ± 1.12	36.14 μm ± 1.86	***	ns	***	
Electroretinography	Scotopic	4D	a-wave amplitude ranging from -0.5 to 0.47 $\log(\text{cd.s/m}^2)$	-90.29 μV ± 8.45	-15.71 μV ± 2.2	-49.83 μV ± 3.35	***	**	*
		4D	b-wave amplitude ranging from -0.5 to 0.47 $\log(\text{cd.s/m}^2)$	297.6 μV ± 16.81	43.83 μV ± 1.5	140.3 μV ± 7.24	***	***	**
	Photopic	4E	b-wave amplitude	79.63 μV ± 6.06	40.88 μV ± 9.89	43.63 μV ± 7.85	***	*	ns
		4F	b-wave implicit time	53.38 ms ± 0.90	61.88 ms ± 3.77	57.13 ms ± 1.92	*	ns	*

Supplemental Table 1: Statistic analysis of histological and electrophysiological parameters of rats treated before light-exposure.

Each line represents mean values of parameters measured in figure 3 and 4, and statistical analysis with one-way ANOVA, followed with Bonferroni post-test. n=8-10; *p<0.05; ** p<0.01; *** p<0.001; ns=not significant. BLE: Rats injected with BSS and exposed to light (red lines); NLE: Control rats neither injected nor exposed to light (black lines); TfLE: Rats injected with human Tf and exposed to light (blue lines).

Gene	TfLE / BLE	p value
Cytokines		
Chemokines		
<i>Ccl1</i>	-2,75	0,335
<i>Ccl5</i>	2,08	0,05
<i>Ccl6</i>	3,09	0,047
<i>Ccl11</i>	1,64	0,217
<i>Ccl20</i>	1,94	0,291
<i>Ccl21</i>	1,52	0,417
<i>Ccl22</i>	2,75	0,244
<i>Ccl24</i>	1,68	0,509
<i>Cxcl3</i>	2,14	0,005
<i>Cxcl5</i>	2,48	0,039
<i>Cxcl9</i>	2,88	0,071
Interleukins		
<i>Il1b</i>	4,33	0,086
<i>Il5</i>	2,72	0,143
<i>Il6</i>	1,57	0,278
<i>Il9</i>	3,79	0,033
<i>Il17a</i>	1,88	0,208
<i>Il22</i>	-1,78	0,027
Others inflammatory molecules		
<i>Faslg</i>	-1,68	0,049
<i>lfng</i>	-4,17	0,309
<i>Lta</i>	1,59	0,322
Receptors		
<i>Ccr1</i>	1,84	0,436
<i>Ccr3</i>	7,78	0,113
<i>Ccr7</i>	1,51	0,952
<i>Cxcr2</i>	4,03	0,197
<i>Cxcr4</i>	1,76	0,188
<i>Il1rap</i>	-1,72	0,011
<i>Il1rn</i>	2,84	0,193
<i>Il8ra</i>	1,98	0,042
<i>Il23r</i>	-2,27	0,044
Signalisation		
<i>Itgb2</i>	1,75	0,204
<i>Tollip</i>	1,55	0,268
<i>Tlr1</i>	1,54	0,54
<i>Tlr5</i>	-2,56	0,309

Supplemental Table 2: Inflammatory genes expression regulated by transferrin treatment.

Results are presented as the average fold change in gene expression obtained in rats injected with transferrin and light-exposed (TfLE) compared to those treated with BSS (TfLE/BLE). Only genes up-regulated (blue) and down-regulated (red) more than 1.5 fold were represented. Significant differences determined with Student's t-test ($p < 0.05$; $n = 5-6$ retinas per group) were bold.

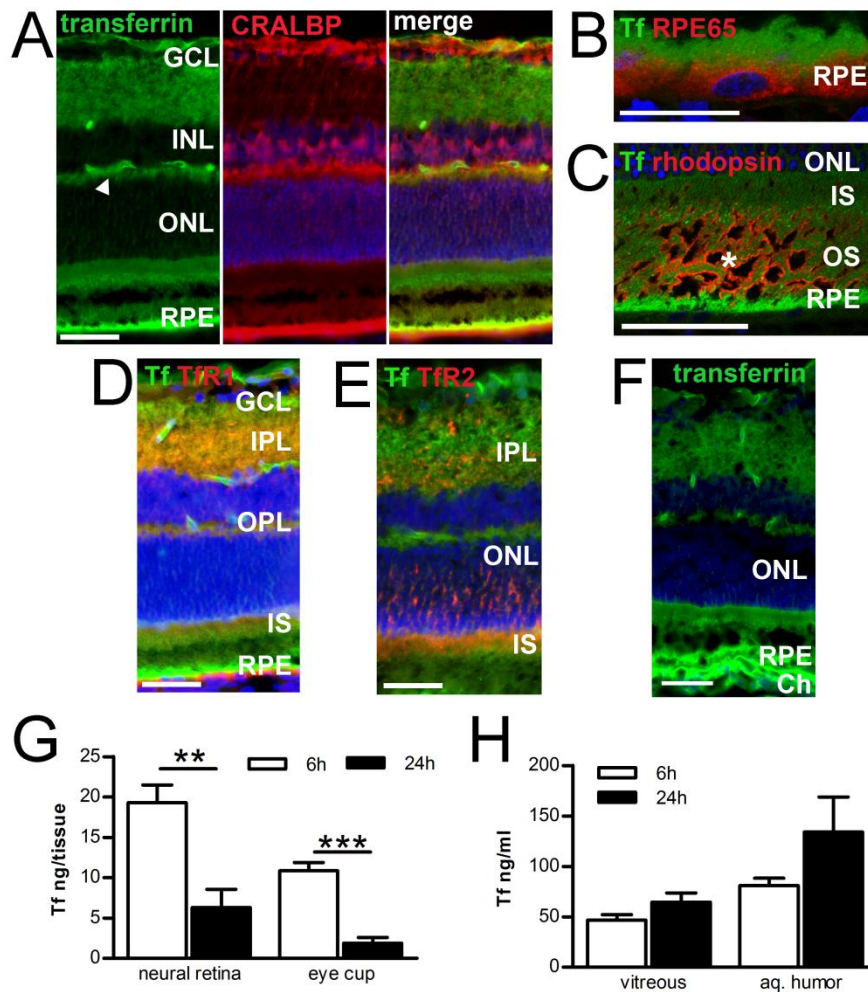


Figure 1: Time-related distribution of transferrin after intravitreal injection in normal rats.

(A-E) Adult Wistar rat received one intravitreal injection of transferrin (Tf) labeled with fluorochrom Alexa 488 (green). (A) Two hours after injection, Tf-Alexa 488 (left) co-localized (right) with Müller glial cells stained with anti-cellular retinaldehyde-binding protein (CRALBP) antibody (middle). (B-C) Higher magnification revealed Tf-Alexa on apical side of retinal pigment epithelium revealed with anti-RPE65 antibody (red) (B), and at photoreceptors segments layers stained with rhodopsin (red, asterisk) (C). (D) Tf-Alexa merged (yellow) with transferrin receptor 1 (red) in synaptic layers. (E) Tf-Alexa co-localized with transferrin receptor 2 (red) in inner segments, outer nuclear layer and inner plexiform layer. (F) Six hours after injection, Tf-Alexa was in overall retina and additionally detected in choroid (Ch) vessels. (G-H) Transferrin levels were quantified in posterior segment tissues (G) and ocular fluids (H) by ELISA assay, 6 and 24 hours after Tf injection. All values are represented as mean± SEM. Student's t-test; n=3-4 rats per time; ** p=0.0032; *** p<0.0001.

Ch: Choroid; GCL: Ganglion cell layer; INL: Inner nuclear layer; IPL: Inner plexiform layer; IS: Inner segment; ONL: Outer nuclear layer; OPL: Outer plexiform layer; OS: Outer segment; RPE: retinal pigment epithelium. Scale bars A, C, D-F: 50µm; B: 20µm. Nuclei stained with DAPI (blue).

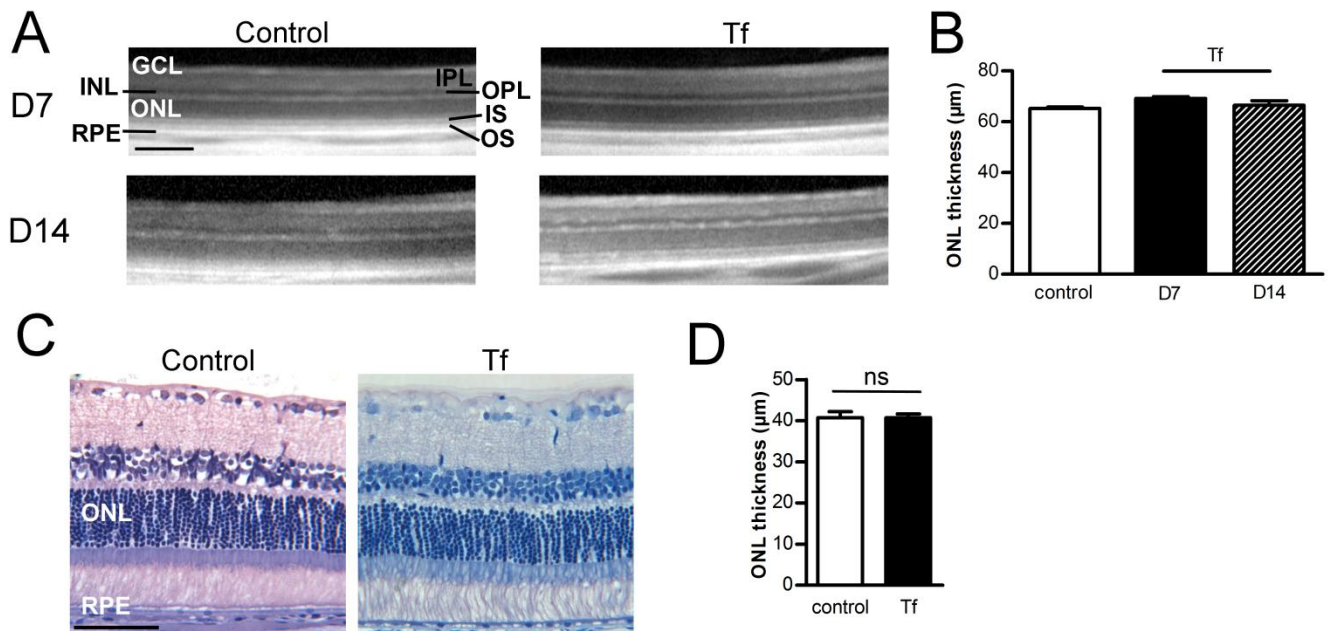


Figure 2: IVT injections of transferrin have no retinal toxicity. (A) *In vivo* retinal structure recorded by optical coherence tomography (OCT) 7 days after first transferrin (Tf) IVT injection (D7) and 7 days after the second Tf injection (D14) in rats, demonstrated no retinal histological modifications. (B) Measurement of outer nuclear layer (ONL) from OCT pictures in control not injected rats and rats injected once (D7) or twice (D14) with Tf. (C) Pictures of historesin semi-thin sagittal retinal sections 7 days after the second Tf injection. (D) Mean ONL thickness measured on sections crossing the optic nerve in overall retina of control rats and twice Tf-injected rats. All values are represented as mean \pm SEM; Student's t-test; n=4 eyes per group; ns= not significant. GCL: Ganglion cell layer; INL: Inner nuclear layer; IPL: Inner plexiform layer; IS: Inner segment; ONL: Outer nuclear layer; OPL: Outer plexiform layer; OS: Outer segment; RPE: retinal pigment epithelium. Scale bar A: 200µm; C: 100µm.

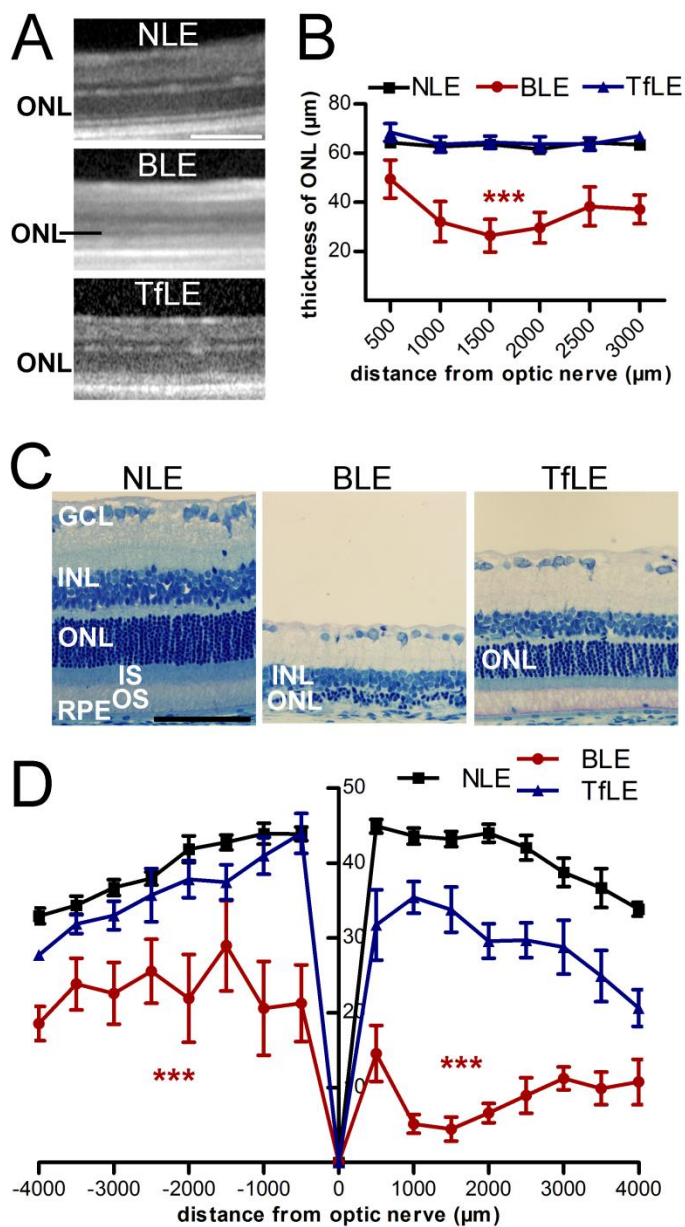


Figure 3: Intravitreal injection of transferrin protects rat retina against light-induced retinal degeneration.

Transferrin (Tf) was injected in rats before a 24-hours continuous light exposure, analyses were performed after 8 days. **(A)** *In vivo* optical coherence tomography (OCT) images showed a reduction of outer nuclear layer (ONL) thickness in BLE rats compare to NLE and TfLE rats. **(B)** ONL thickness of superior pole (500 to 3,000 μm from optic nerve) measured on OCT pictures in intervals of 500 μm , in NLE, BLE and TfLE rats. **(C)** Retinal semi-thin sections at the superior pole showed important photoreceptor nuclei layer (ONL) degeneration in BLE rats as compared to control (NLE) or TfLE rats. **(D)** Measures of ONL thickness, with intervals of 500 μm , across the entire retina show that Tf-treatment significantly protect photoreceptors nuclei layer thickness as compared to BSS treatment.

BLE: Rats injected with BSS and exposed to light (red lines); NLE: Control rats neither injected nor exposed to light (black lines); TfLE: Rats injected with human Tf and exposed to light (blue lines). All values are represented as mean \pm SEM; One-way ANOVA, followed with Bonferroni post-test. n=8-10 eyes per group; significant differences (***) $p < 0.001$ were observed between TfLE and BLE. All statistic analyses can be found in Supp. Table 1. GCL: Ganglion cell layer; INL: Inner nuclear layer; IS: Inner segment; ONL: Outer nuclear layer; OS: Outer segment; RPE: retinal pigment epithelium. Scale bars: A: 200 μm , C: 100 μm .

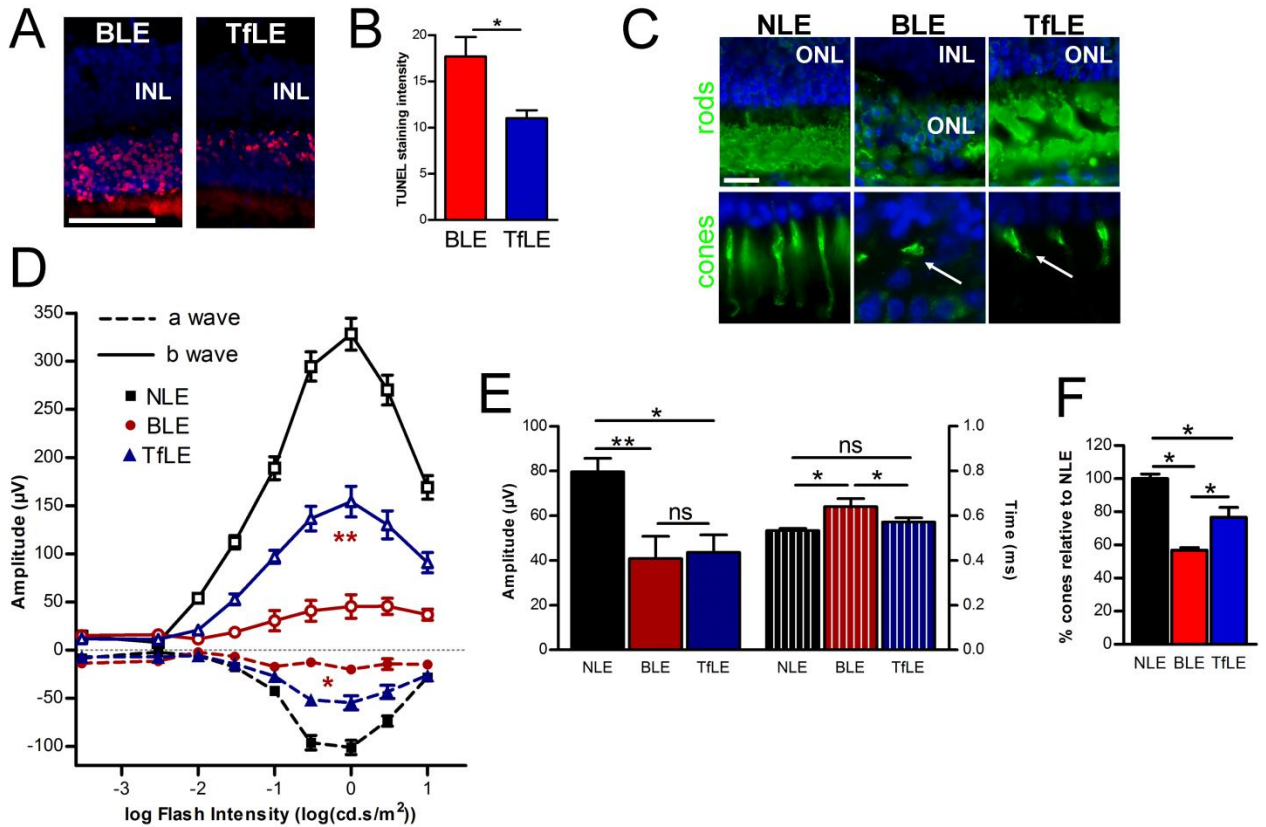


Figure 4: Transferrin decreases light-induced photoreceptors apoptosis and preserves visual activities. (A) TUNEL staining (red) and (B) fluorescence intensity quantification at the photoreceptors nuclei layer, 1 day after light exposure show a reduction of apoptosis in TfLE compared to BLE retinas. Mann-Whitney test; $n=3-4$ retinas per group; $*p=0.0201$. (C) Rods immunostaining (green, top panel) and cones lectin staining (green, bottom panel, arrows) in rats at 8 days reflect the integrity of TfLE photoreceptors. (D) Scotopic electroretinogram, specific to rod-driven responses, was recorded 16 days after light exposure. Light (red lines) induced a collapse of a-waves (dotted lines) and b-waves (solid waves) amplitudes. Those amplitudes were preserved in TfLE (blue lines) and reached nearly 50% of NLE values (black lines). One-way ANOVA, followed with Bonferroni post-test. $n=8$ eyes per group; significant differences ($*p<0.05$, $**p<0.01$) were observed between TfLE and BLE. (E) Photopic ERG was recorded after saturation of rods to obtain specific cone response. The amplitude (left part) and the implicit time (right part) of the b-wave are represented on the graph. While the light induced reduction of the b-wave amplitude was not prevented by the injection of Tf (blue bar), the treatment normalized the b-wave implicit time (shaded blue bar). One-way ANOVA, followed with Bonferroni post-test. $n=8$ eyes per group; significant differences ($*p<0.05$, $**p<0.01$). (F) Quantification of cones on superior pole. BLE group and TfLE are expressed relative to the control group (NLE). Percentage of cones reduced in BLE rats was partially preserved in TfLE rats. Mann-Whitney t-test; $n=3$ eyes per group; $*p<0.05$. BLE: Rats injected with BSS and exposed to light (red); NLE: Control rats neither exposed to light, neither injected (black); TfLE: Rats injected with human Tf and exposed to light (blue). All values are represented as mean \pm SEM. (Complete statistic analysis for D and E can be found in Supp. Table 1. INL: Inner nuclear layer; ONL: Outer nuclear layer. A, C: Nuclei stained with DAPI. Scale bars A: $100\mu\text{m}$; C: $20\mu\text{m}$.)

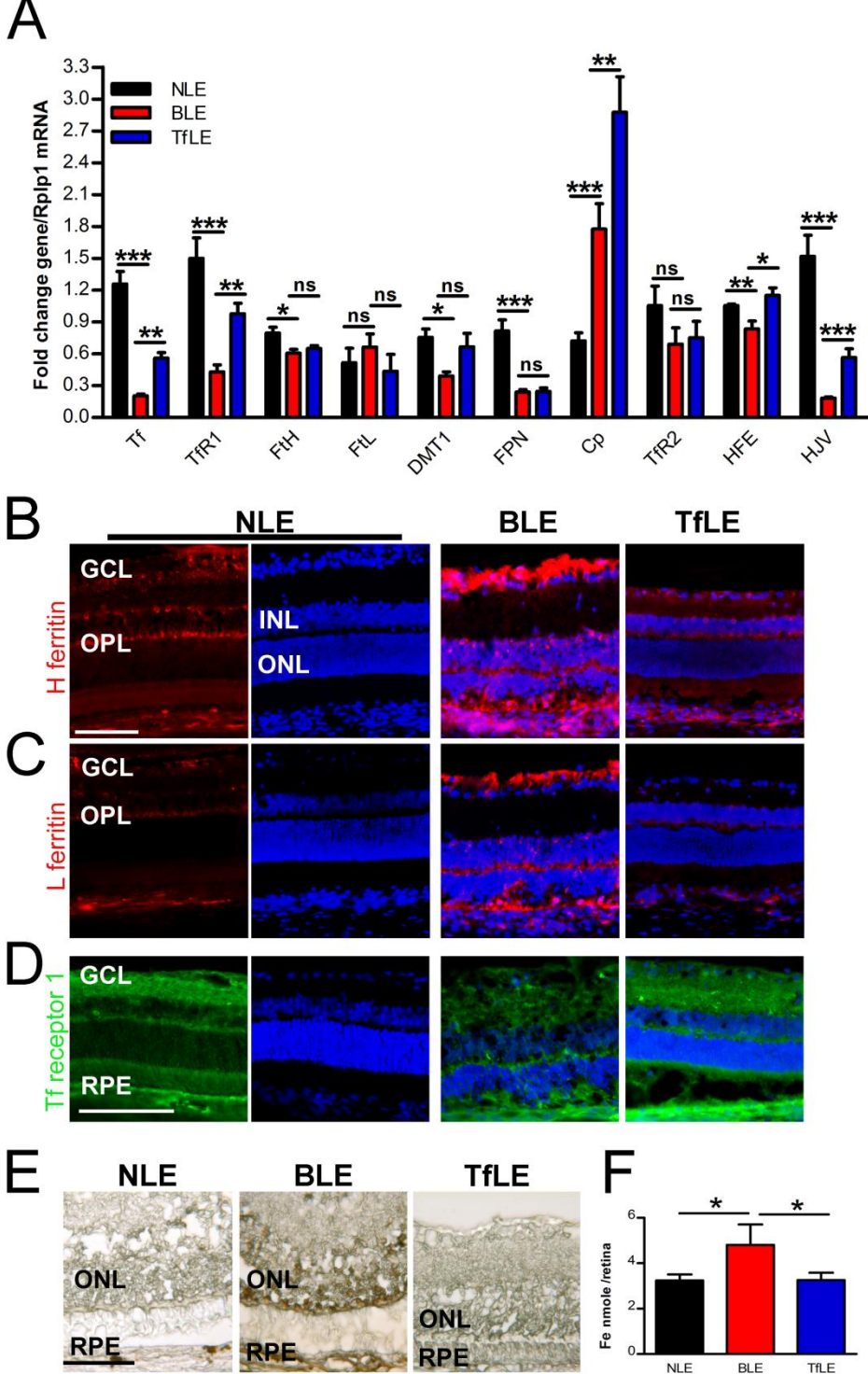


Figure 5: Transferrin treatment controls iron metabolism.

(A) Quantitative PCR of iron-related genes mRNA normalized with Ribosomal Protein P1 (*Rplp1*) mRNA on neural retina one day after light exposure. Transcripts related to transport (*Tf* and *TfR1*), storage (Ferritin Heavy chain (*Fth*) and Light chain (*FtL*)), export (Divalent metal transporter 1 (*Dmt1*), Ferroportin (*Fpn*), Ceruloplasmin (*Cp*)) and regulation of iron (*TfR2*, Human hemochromatosis protein (*Hfe*), Hemojuvelin (*Hjv*)) were modified following light exposure when comparing BLE to NLE rats. When comparing TfLE to BLE retinas, Tf-treatment modulated the expression of several of these iron-related mRNAs. All values are represented as mean \pm SEM; One-way ANOVA, Bonferroni post-test; $n=5-6$ neural retinas; * $p<0.05$; ** $p<0.01$; *** $p<0.001$, ns= not significant. **(B-D)** Immunohistochemistry of ferritins and transferrin receptor 1 on retinal sections 3 days after light exposure. Heavy chain (B) and light chain (C) ferritins and transferrin receptor 1 staining (D) were conserved in TfLE rat retinas (right column) as compared to NLE rat retinas (left column), whereas proteins staining intensities were modified in BLE rat retinas (central column). Nuclei stained with DAPI (blue). Scale bar B-D: 100 μ m. **(E)** Iron labeling on retinal cryosections demonstrate iron accumulation in outer retinas of BLE rats at 8 days after light exposure. TfLE retinas iron staining was similar to NLE rat retinas. Scale bar: 100 μ m. **(F)** Total non-heme iron quantification in the retinas demonstrate that Tf prevented free iron content to increase after light exposure. All values are represented as mean \pm SEM; Kruskal-Wallis, Dunn post-test; $n=3-4$ retinas; * $p<0.05$. BLE: Rats injected with BSS and exposed to light (red); NLE: Control rats neither injected nor exposed to light (black); TfLE: Rats injected with human Tf and exposed to light (blue).

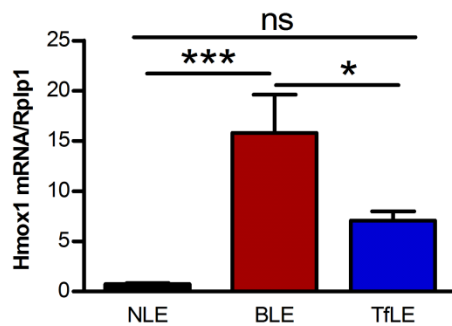


Figure 6: Transferrin inhibits light-induced oxidative stress.

Heme oxygenase 1 (*Hmox1*) mRNA expression related to control gene Ribosomal Protein P1 (*Rplp1*) was determined in neural retina one day after light-injury. While light exposure drastically increases *Hmox1* gene expression (BLE group), Tf injection significantly reduced this increase (TfLE group). All values are represented as mean of fold change \pm SEM. One-way ANOVA, Bonferroni post-test; n=5-6 retina per group; *p<0.05; *** p<0.001; ns = not significant. BLE: Rats injected with BSS and exposed to light (red bar); NLE: Control rats neither injected nor exposed to light (black bar); TfLE: Rats injected with human Tf and exposed to light (blue bar).

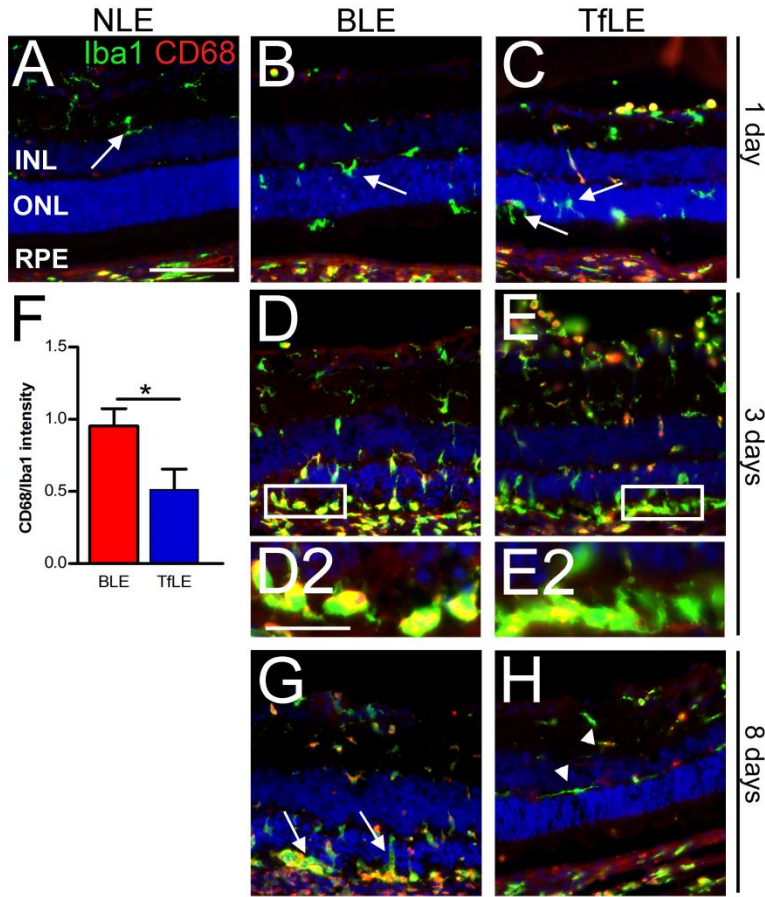


Figure 7: Transferrin injection manages inflammatory cells responses.

(A) In control group, microglia cells (arrow) anti-ionized calcium binding adaptor molecule 1 (Iba1) positive were localized in inner retina and negative for anti-CD68, marker of activation. (B-G) Microglial/macrophages cells migrated in photoreceptors layer (arrows) after light-exposure as observed 1 (B-C), 3 (D-E) or 8 (G-H) days after light period. (D2-E2) Higher magnification of corresponding area delimited in outer retina of D and E revealed more Iba1+/CD68+ co-staining in BLE rats than in TfLE rats. (F) Quantification of CD68 positive cells staining were reported to Iba1 cells intensity staining measured in outer retina 3 days after light period. Microglial/macrophages activation after light exposure was reduced with Tf injection. All values are represented as mean± SEM. Mann-Whitney test; n=3 eyes per time; *p=0.0104. (G-H) At day 8, in BLE rat retinas, microglial/macrophages cells accumulated in outer retina (arrows, G) compared to TfLE retinas (arrowheads, H).

Rats injected with BSS and exposed to light (red bar); TfLE: Rats injected with human Tf and exposed to light (blue bar). Scale bar A-H: 100µm; D2-E2: 50µm.

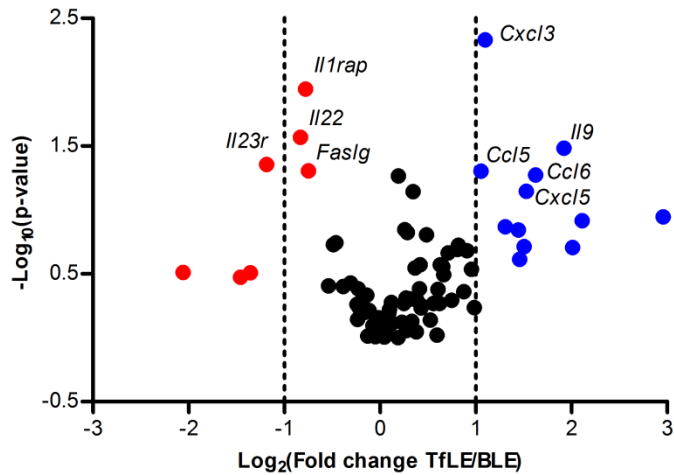


Figure 8. Volcano plots of mRNAs regulated by transferrin in light exposed retinas.

Volcano plot of 84 differentially expressed genes in light exposed retinas treated with Tf relative to control treatment ($n = 5-6$ per group) according to their p-value versus fold change. Highest fold change expression ($|\text{Log}_2^{\text{(fold change)}}| \geq 2$) are colored. Significant differences were determined with Student's t-test ($p < 0.05$; $n = 5-6$ retinas per group). BLE: Rats injected with BSS and exposed to light (red bar); TfLE: Rats injected with human Tf and exposed to light (blue bar).

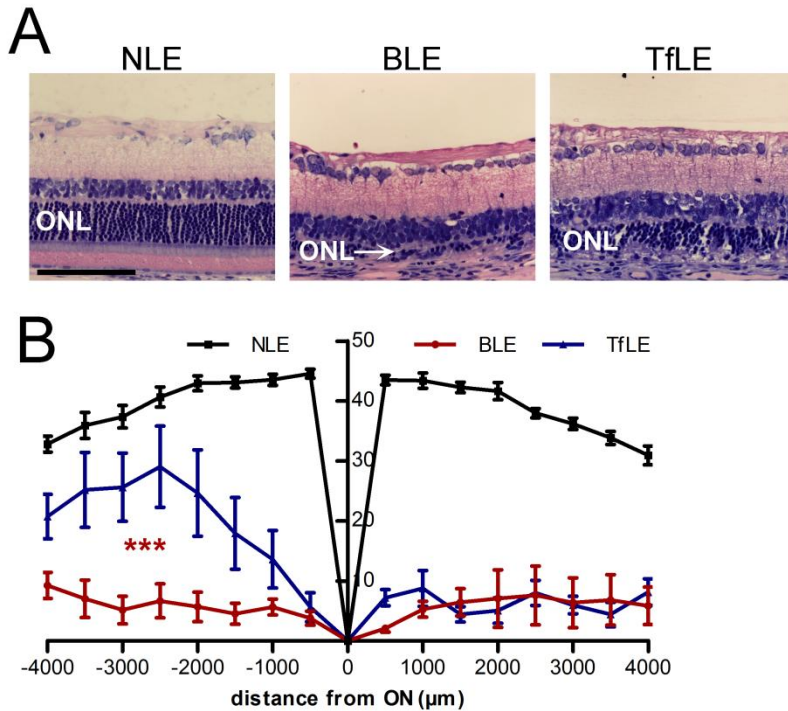


Figure 9: Intravitreal injection of transferrin partially protects degenerated retina.

After a dark adaptation period, rats were placed under a 24-hour intense light treatment. We subsequently injected Tf or BSS solutions via IVT, and sacrificed them 8 days later. **(A)** Histoiresin blue-stained sections on inferior pole demonstrate partial preservation of retina structure with Tf injection. ONL: Outer nuclear layer. Scale bar: 100 μm . **(B)** ONL thickness measurement throughout the retina, every 500 μm , showed protective effect of Tf only in the inferior pole. All values are represented as mean \pm SEM; TfLE retinas were compared to BLE at each different distance from the optic nerve with one-way ANOVA, Bonferroni post-test; $n=8$ eyes per group; *** $p<0.001$. BLE: Rats injected with BSS and exposed to light (red line); NLE: Control rats neither injected nor exposed to light (black line); TfLE: Rats injected with human Tf and exposed to light (blue line).

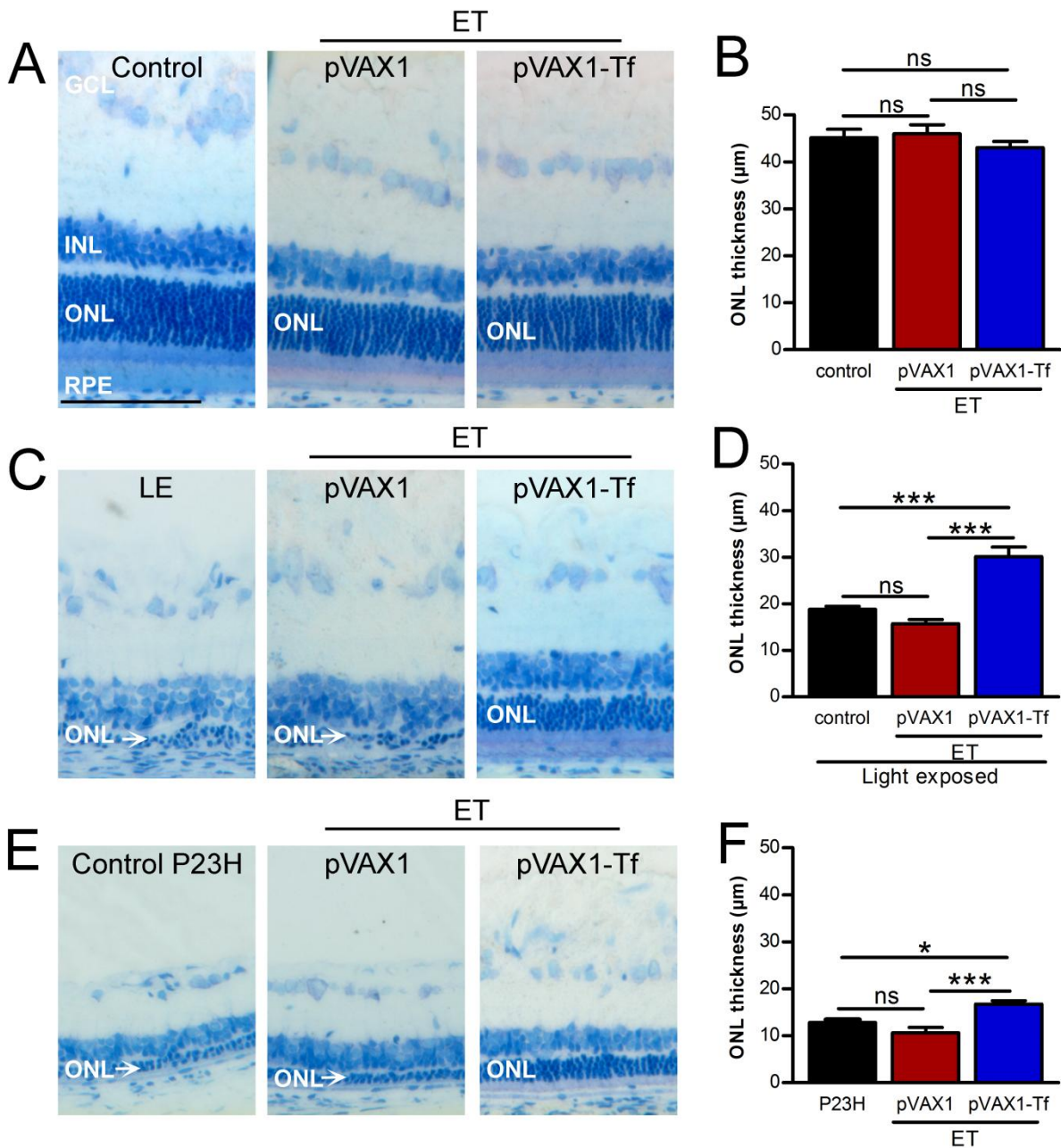


Figure 10: Non-viral gene therapy for local transferrin production preserves photoreceptors in 2 models of retinal degeneration.

(A) Histology of the retina following electrotransfer of empty plasmid (pVAX1) or containing cDNA of transferrin (pVAX1-Tf). **(B)** Mean ONL thickness evaluated on histoiresin semi-thin retinal sections in control rats (black bar), and 12 days after ET of pVAX1 (red bar) or pVAX1-Tf (blue bar) in rats. ET and substained production of Tf had no deleterious effect on retina structure. **(C)** Histoiresin sections **(D)** and mean of ONL thickness of rats electrotransferred with pVAX1 (red bar) or pVAX-Tf (blue bar), submitted to light-exposure (LE) 3 days after, and sacrificed 8 days later. Control rats not ET but exposed to light are represented with black bar (control, LE). **(E)** Histoiresin sections and mean of ONL thickness **(F)** of P23H rats retinas (black bar), model of slow retinal degeneration, electrotransferred at 4 weeks of age with pVAX1 (red bar) or pVAX-Tf plasmids (blue bar), and sacrificed 4 weeks later. Scale bar: 100µm; All values are represented as mean ±SEM; One-way ANOVA, Bonferroni post-test; n=6-10 eyes per group; *p<0.05; ***p<0.001; ns=not significant.

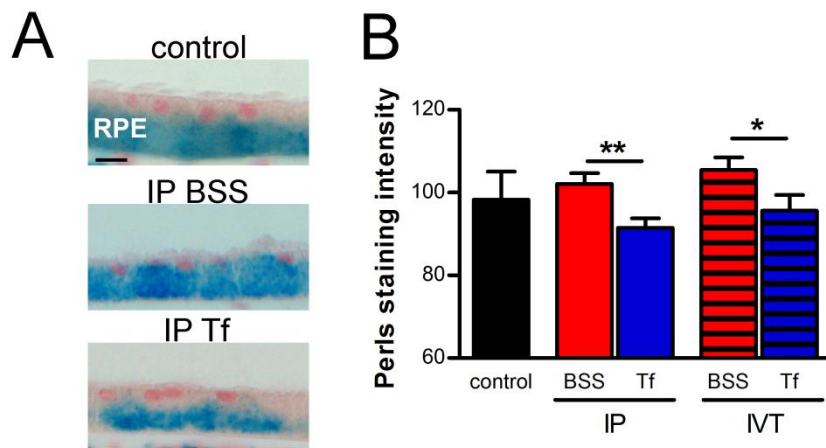
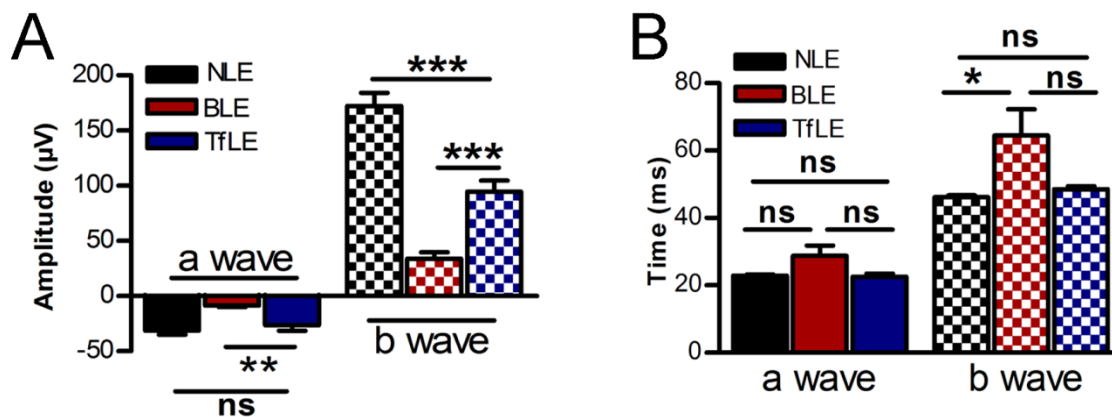


Figure 11: Treatments with transferrin remove retinal iron deposits in a mouse model of iron overload.

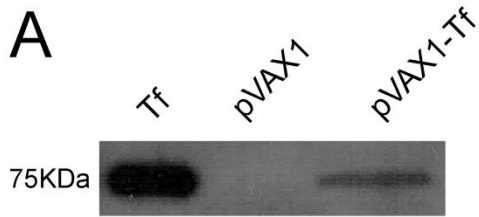
(A) Iron staining (blue) by Perls method in the RPE of 32 weeks-old mice *Bmp6*^{-/-} (control), intraperitoneally (IP) injected with BSS or Tf. Sections were counterstained with nuclear red. RPE: Retinal pigment epithelium. Scale bar: 10 μ m. **(B)** Quantification of iron staining in retinal pigment epithelium (RPE) in 32 weeks-old *Bmp6* KO mice (black bar), treated with Tf (blue bar) or BSS (red bar) by IP injections, 3 times per week for one month, or with a single intravitreal injection. All values are represented as mean \pm SEM; Student's t-test; n=4-6 retinas per group; *p=0.0475; **p=0.0035



Supplementary Figure 1: Supplementary electroretinograms recording confirm partial preservation of retinal functions following transferrin injection.

Mixed (rods+cones-driven responses) ERG were recorded 16 days after light-exposure. Negative a-waves represent photoreceptors responses and positive b-waves are relevant for post-receptor responses. **(A)** As light-exposure induced a drastic collapse of the mixed a- and b-waves amplitudes, Tf injection significantly preserved nearly 50% of physiological responses of the retina. **(B)** Light exposure increased a- and b-waves implicit times (time of stimulus to peak time), and Tf injection normalized both values. All values are represented as mean \pm SEM. One-way ANOVA, Bonferroni post-test; n=8 eyes per group; * p<0.05; ** p<0.01; *** p<0.001.; ns: not significant.

BLE: Rats injected with BSS and exposed to light (red bars); NLE: Control rats neither injected nor exposed to light (black bars); TfLE: Rats injected with human Tf and exposed to light (blue bars).



B

	mean	std error
vitreous	7.60	2.28
humor aq.	4.37	1.46
retina	0.03	0.02
eye cup	0.16	0.09

Supplementary Figure 2: Analysis of transferrin produced after electrotransfer

(A) Western blot analysis of transferrin (Tf) expression in ARPE-19 cell culture medium 3 days after transfection with control empty plasmid (pVAX1) or a plasmid containing human Tf cDNA (pVAX1-Tf). Positive control was done by culture cell medium added with Tf extracted from human plasma. **(B)** human Tf-ELISA assay was performed on vitreous and aqueous humor (ng/ml), and in neural retinas and eye cups (ng/tissue), 3 days after electrotransfer (ET) of pVAX1-Tf plasmid in rats. All values are represented as mean \pm SEM; n=3-4 rats per group.

Supplementary Material and legends

[Click here to download Supplementary Material: Supplemental methods and legends article emilie VF2.docx](#)